Soft Computing (2021) 25:7435–7457
https://doi.org/10.1007/s00500-021-05705-5

METHODOLOGIES AND APPLICATION

Modeling, analysis and real-time implementation of five new simplest fuzzy nonlinear PI/PD controllers

Debdoot Sain[1] · **B. M. Mohan**[1]

Accepted: 17 February 2021 / Published online: 17 March 2021

Abstract
In spite of accuracy, but due to computational complexity, Center of Gravity (CoG) defuzzification remained dormant for the mathematical modeling of fuzzy controllers for a long time in the past. Recently, Arun and Mohan (ISA Trans 70:16–29, 2017) obtained the mathematical models of two simplest fuzzy PI/PD controllers using CoG defuzzification. In this study, the mathematical models of another five simplest fuzzy PI/PD controllers are obtained, and their properties and computational aspects are investigated. Sufficient conditions for Bounded-Input-Bounded-Output stability of a closed-loop system containing one of these controllers in the loop are also established using the Small-Gain theorem. To justify the theoretical developments made in this manuscript, the applicability of the controllers is shown in simulation and real-time.

Keywords Simplest fuzzy PI/PD controller · Mathematical modeling · Stability analysis · Computational aspects · Center of gravity defuzzification · Larsen product inference · Real-time implementation

1 Introduction

Since inception, fuzzy logic has been a topic of significant interest to the scientific community, and over the years, it has been applied successfully in different fields of research. Control practitioners and the field of control systems engineering are no exception to this. The merit of fuzzy logic controllers lies in their ability to control ill-defined plants. By ill-defined, we mean those systems which can not be represented by a set of differential equations (for continuous-time systems) or difference equations (for discrete-time systems). From literature, it appears to the authors that in most cases, fuzzy logic controllers can provide improved response or at least comparable response as compared to other control strategies. Though the use of fuzzy logic is prominent in the field of control systems engineering since 1970s, unfortunately, till 1990, no specific mathematical model was available for the fuzzy logic controllers. The development of systematic mathematical approaches for fuzzy logic control systems is still on-going, and there is a wide scope to explore. This is indeed the primary motivation for us to consider this field as our area of research.

The concept of fuzzy sets was introduced by Zadeh (1965) in 1965, and in 1972, the same author highlighted the significance of fuzzy algorithms for the control of ill-defined large man-machine systems (Zadeh 1972). In the same paper, the author argued that to provide a suitable environment for the advancement of fuzzy algorithms, control theory must become less preoccupied with mathematical rigor and exactness, and more stress should be given to the advancement of qualitative or approximate solutions to solve the real-world control problems. Motivated by this, the very first application of the fuzzy set theory was reported by Mamdani (1974) in 1974, where a laboratory-built steam engine was controlled. In the same paper, the author indicated that fuzzy logic-based controllers would be useful in controlling the ill-defined plants, such as those present in the process plants like cement, chemical, iron, and steel industries. After Mamdani's pioneering work, fuzzy logic controllers were extensively used to provide solutions to various control engineering problems. While the application of fuzzy logic was prominent in the field of control systems, the underlying theory and the mathematical models of fuzzy controllers were not clear for a long time. The scenario started to change while the first mathematical model of a fuzzy PI controller appeared

✉ Debdoot Sain
saindebdoot@iitkgp.ac.in

B. M. Mohan
mohan@ee.iitkgp.ac.in

[1] Department of Electrical Engineering, Indian Institute of Technology, Kharagpur, Kharagpur 721302, India

in 1990 (Ying et al. 1990). This controller is termed as 'the simplest' fuzzy controller as it employs minimum number of fuzzy sets on the input and output variables. Subsequently, by following the same basic approach, three more models of the simplest fuzzy PI controller were found by Ying (1993). Malki et al. (1994) found the mathematical model of the simplest fuzzy PD controller. It will not be an exaggeration to say that these research works (Ying et al. 1990; Ying 1993; Malki et al. 1994) prepared the base for the subsequent developments of mathematical models of fuzzy logic controllers. Mathematical models of few other simplest fuzzy PD (Mohan and Patel 2002) and PI (Patel and Mohan 2002) controllers were derived by Mohan and Patel using different $t-$norms, $t-$conorms (also known as s-norms), inference methods, and Center of Sums (CoS) defuzzification. From all these papers, it is clear that fuzzy controllers do not have a single fixed model. Depending on the choice of membership functions, $t-$norms, $t-$conorms, inference methods, and defuzzification strategies, different models are possible, and each model is unique in terms of its control ability. In subsequent years, this particular aspect of fuzzy controller modeling motivated many researchers to develop new mathematical models of fuzzy PI/PD controllers (Haj-Ali and Ying 2003; Mohan and Sinha 2008; Neelimegham and Bosukonda 2015; Arun and Mohan 2017). Apart from type-1 fuzzy PI/PD controllers, presence of interval type-2 fuzzy PI/PD controllers (Du and Ying 2010; Nie and Tan 2012; Yip et al. 2019; Zhou et al. 2002) can also be noticed in the literature. Though interval type-2 fuzzy controllers are becoming popular day by day, there is still an ample scope to explore the mathematical models of type-1 fuzzy controllers. This is because type-1 fuzzy controllers are computationally simpler than interval type-2 fuzzy controllers. For the mathematical modeling of Takagi-Sugeno type fuzzy PI/PD controllers, one may refer to Raj and Mohan (2019), Raj and Mohan (2020).

It can be observed from the literature that except Arun and Mohan, no one has found the mathematical models of the simplest fuzzy PI/PD controllers using CoG defuzzification (Arun and Mohan 2017) till date. Though CoG defuzzification is more accurate as compared to the CoS defuzzification, because of computational simplicity the CoS defuzzification is more popular in finding the mathematical models of fuzzy controllers. As CoG defuzzification offers more accurate mathematical models of fuzzy controllers, in this study, we aim to find the mathematical models of the simplest fuzzy PI/PD controllers via CoG defuzzification. Without further ado, let us now state the overall objective of the present study.

In this study, our aim is to reveal the analytical structures of five new simplest fuzzy PI/PD controllers using different t-norms (Algebraic Product (AP) and Minimum (Min)) and t-conorms (Bounded Sum (BS), Algebraic Sum (AS) and Maximum (Max)), Larsen Product (LP) inference and CoG defuzzification. The proposed classes of the simplest fuzzy PI/PD controllers developed in this study are summarized in Table 1.

Table 1 Proposed classes of fuzzy PI/PD controllers

Class	t-norm	t-conorm
1	AP	BS
2	AP	AS
3	Min	BS
4	Min	AS
5	Min	Max

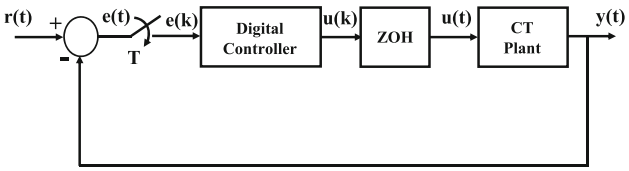

Fig. 1 Block diagram of a computer control system

The analytical structure of the Class 6 controller using AP t-norm, Max t-conorm, LP inference and CoG defuzzification was already obtained by Arun and Mohan (2017). The properties and computational aspects of the proposed simplest fuzzy PI/PD controllers are addressed and sufficient conditions for the BIBO stability of a closed loop system containing one of these controllers in the loop are established using the Small-Gain theorem. To justify the theoretical development made in this manuscript, the applicability of proposed fuzzy controllers is depicted by considering two simulation examples and two real-time studies. Moreover, performances of the proposed controllers are compared for better understanding.

This manuscript is organized into nine sections. In Sections 2 and 3, details of the conventional PI/PD controllers and the principal components of the simplest fuzzy PI/PD controllers are provided, respectively. Analytical structures, BIBO stability and computational aspects of the proposed fuzzy controllers are discussed in Sections 4, 5 and 6. The applicability of newly found controllers is depicted through simulation and real-time studies on a few nonlinear plants in Sections 7 and 8. Conclusions of the present study highlighting the future scope of research are presented in Section 9.

2 Conventional discrete-time PI/PD controllers

In Fig. 1, the block diagram of a typical closed loop computer control system is provided, where the plant under control is Continuous-Time (CT) in nature and T represents the sampling period. For brevity, henceforth we drop T from kT and $(k-1)T$.

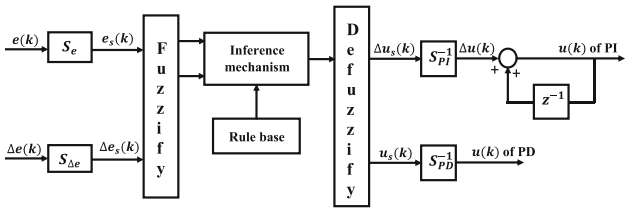

Fig. 2 Block diagram of a typical fuzzy PI/PD controller

The control effort generated by the Discrete-Time (DT) linear PI controller at kth sampling instant is given by

$$u_{\mathrm{PI}}(k) \;=\; u_{\mathrm{PI}}(k-1) + \Delta u_{\mathrm{PI}}(k) \tag{1}$$

where $u_{\mathrm{PI}}(k-1)$ and $\Delta u_{\mathrm{PI}}(k)$ represent the control effort at $(k-1)$th sampling instant and incremental control effort at kth sampling instant, respectively.

In terms of error $e(k)$ and change in error $\Delta e(k)$ (defined as $e(k) - e(k-1)$), the expression for $\Delta u_{\mathrm{PI}}(k)$ is given by

$$\Delta u_{\mathrm{PI}}(k) \;=\; K_P^{dt}\,\Delta e(k) + K_I^{dt}\,e(k) \tag{2}$$

where K_P^{dt} and K_I^{dt}, respectively, represent the proportional and integral gains of DT linear PI controller. In terms of the scaled version of $e(k)$ and $\Delta e(k)$, Eq. (2) can be rewritten as

$$\Delta u_{\mathrm{PI}}(k) \;=\; \Delta \hat{e}_s(k) + \hat{e}_s(k) \tag{3}$$

where $\hat{e}_s(k)$ and $\Delta \hat{e}_s(k)$ represent the scaled version of $e(k)$ and $\Delta e(k)$, respectively, and $\hat{e}_s(k) \;=\; K_I^{dt} e(k)$ and $\Delta \hat{e}_s(k) \;=\; K_P^{dt}\,\Delta e(k)$.

On the other hand, DT linear PD controller output at kth sampling instant is given by

$$u_{\mathrm{PD}}(k) \;=\; K_P^{dt} e(k) + K_D^{dt}\,\Delta e(k) \tag{4}$$

where proportional and derivative gains of DT linear PD controller are represented by K_P^{dt} and K_D^{dt}, respectively. Equation (4) can be rewritten as

$$u_{\mathrm{PD}}(k) \;=\; \tilde{e}_s(k) + \Delta \tilde{e}_s(k) \tag{5}$$

where $\tilde{e}_s(k) \;=\; K_P^{dt} e(k)$, $\Delta \tilde{e}_s(k) \;=\; K_D^{dt}\,\Delta e(k)$, and respectively represent the scaled version of $e(k)$ and $\Delta e(k)$.

3 Basic components of fuzzy PI/PD controllers

The basic block diagram of a typical fuzzy PI/PD controller, depicted in Fig. 2, consists of fuzzification, inference mechanism, rule base, and defuzzification modules.

From the block diagram, it can be observed that like the conventional DT linear PI and PD controllers, the inputs to the fuzzy PI and PD controllers are the scaled version of $e(k)$ and $\Delta e(k)$ i.e., $e_s(k)$ and $\Delta e_s(k)$. The scaled outputs of fuzzy PI and PD controllers are denoted by $\Delta u_s(k)$ and $u_s(k)$, respectively, and they are in general a nonlinear function of $e_s(k)$ and $\Delta e_s(k)$. The nature of nonlinearity depends on the choice of membership functions, t-norms, t-conorms, inference mechanisms and defuzzification strategies. For the purpose of having normalized Universes of Discourse (UoDs), input normalization and output denormalization are required and they are achieved by using scaling factors. In Fig. 2, the scaling factors of the simplest fuzzy PI/PD controllers are represented by S_e, $S_{\Delta e}$, S_{PI}^{-1} and S_{PD}^{-1}. S_e and $S_{\Delta e}$ are responsible for input normalization and S_{PI}^{-1} (for PI controller) and S_{PD}^{-1} (for PD controller) take care of output denormalization. The details of the principal components of the simplest fuzzy PI/PD controllers are presented in the following subsections.

3.1 Fuzzification

For the fuzzy sets on scaled input variables, L and Γ types of membership functions (Driankov et al. 1993) are considered and depicted in Fig. 3. The purpose of using the fuzzification module is to convert the crisp values of the scaled process variables into fuzzy variables to make them compatible with the fuzzy set representation of the scaled process variables used in the control rule base. The mathematical description of the input membership functions is as follows:

$$\mu_{E^{-1}}(e_s(k)) = \begin{cases} 1 & \text{if } e_s(k) \le -h_e \\ \frac{-e_s(k)+h_e}{2h_e} & \text{if } -h_e \le e_s(k) \le h_e \\ 0 & \text{if } h_e \le e_s(k) \end{cases}$$

$$\mu_{E^{+1}}(e_s(k)) = \begin{cases} 0 & \text{if } e_s(k) \le -h_e \\ \frac{e_s(k)+h_e}{2h_e} & \text{if } -h_e \le e_s(k) \le h_e \\ 1 & \text{if } h_e \le e_s(k) \end{cases}$$

$$\mu_{\Delta E^{-1}}(\Delta e_s(k)) = \begin{cases} 1 & \text{if } \Delta e_s(k) \le -h_{\Delta e} \\ \frac{-\Delta e_s(k)+h_{\Delta e}}{2h_{\Delta e}} & \text{if } -h_{\Delta e} \le \Delta e_s(k) \le h_{\Delta e} \\ 0 & \text{if } h_{\Delta e} \le \Delta e_s(k) \end{cases}$$

$$\mu_{\Delta E^{+1}}(\Delta e_s(k)) = \begin{cases} 0 & \text{if } \Delta e_s(k) \le -h_{\Delta e} \\ \frac{\Delta e_s(k)+h_{\Delta e}}{2h_{\Delta e}} & \text{if } -h_{\Delta e} \le \Delta e_s(k) \le h_{\Delta e} \\ 1 & \text{if } h_{\Delta e} \le \Delta e_s(k) \end{cases}$$

Different UoDs for the input variables are considered as the maximum values of $|e_s(k)|$ and $|\Delta e_s(k)|$ are usually unequal (Braae and Rutherford 1979). For the fuzzy sets on

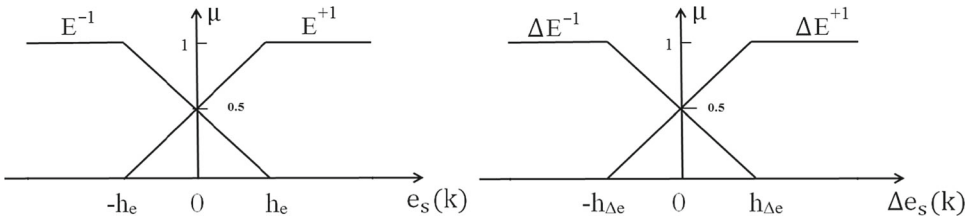

Fig. 3 Membership functions of fuzzy sets on the scaled input variables

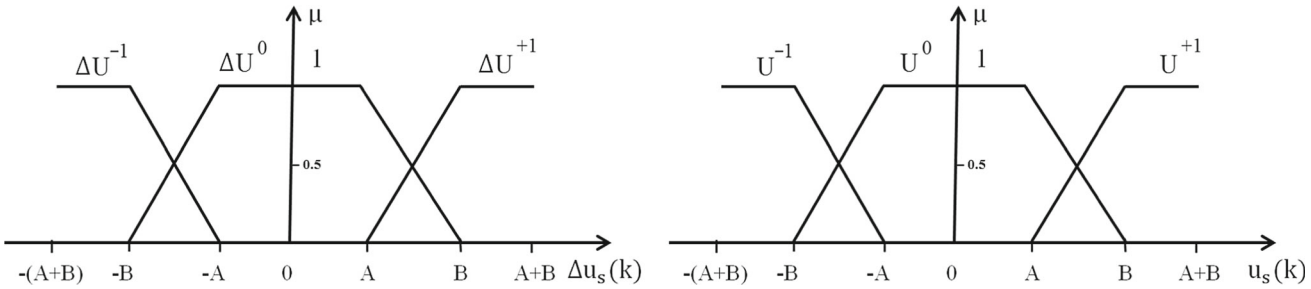

Fig. 4 Membership functions of fuzzy sets on the scaled output variable

the scaled output variable, L, Π, and Γ types of membership functions are considered and shown in Fig. 4. Note that the sum of membership functions of the fuzzy sets on the scaled input and output variables at any point over the UoD is unity. For computational simplicity, in some earlier works only Π-type membership functions were considered for the fuzzy sets on the scaled output variable and their sum at some points in the UoD is not unity. The parameter A of the fuzzy set on the output variable can take any value in $[0, B)$. Under the condition $A = 0$, the trapezoids in Fig. 4 become a triangle. This means that the analytical structures of the simplest fuzzy PI/PD controllers with L, triangular (Λ) and Γ types of membership functions (on the scaled output variable) can be found by putting $A = 0$ in the expressions of the fuzzy controllers obtained with L, Π, and Γ types of membership functions.

3.2 Rule base

The following four rules have been utilized for building the rule base of the simplest fuzzy PI controller.

R_1 : IF $e_s(k)$ is E^{-1} AND $\Delta e_s(k)$ is ΔE^{-1} THEN $\Delta u_s(k)$ is ΔU^{-1}

R_{2a} : IF $e_s(k)$ is E^{-1} AND $\Delta e_s(k)$ is ΔE^{+1} THEN $\Delta u_s(k)$ is ΔU^{0}

R_{2b} : If $e_s(k)$ is E^{+1} AND $\Delta e_s(k)$ is ΔE^{-1} THEN $\Delta u_s(k)$ is ΔU^{0}

R_3 : IF $e_s(k)$ is E^{+1} AND $\Delta e_s(k)$ is ΔE^{+1} THEN $\Delta u_s(k)$ is ΔU^{+1}

For the most commonly encountered control problems i.e. set-point problems, these four rules should be sufficient as there are only four different scenarios, each of which will be taken care of by one of these rules (Ying 2000). With the help of Fig. 5, the reason behind choosing this rule base is justified. In Fig. 5, $r(k)$, $y(k)$, $e_s(k)$ and $\Delta e_s(k)$ represent unit step input, unit step response, scaled error and scaled change of error, respectively, of a second-order linear time invariant system. From this figure we observe that at any time instant the system response $y(k)$ is either above or below the reference $r(k)$ and either it goes away from or approaches $r(k)$. This actually gives us the following four cases.

Case 1: $y(k)$ is above $r(k)$ and $y(k)$ goes away from $r(k)$ (ex. point P_1 in Fig. 5)

Case 2: $y(k)$ is above $r(k)$ and $y(k)$ approaches $r(k)$ (ex. point P_{21} in Fig. 5)

Case 3: $y(k)$ is below $r(k)$ and $y(k)$ approaches $r(k)$ (ex. point P_{22} in Fig. 5)

Case 4: $y(k)$ is below $r(k)$ and $y(k)$ goes away from $r(k)$ (ex. point P_3 in Fig. 5)

In these four cases the signs of $e_s(k)$ and $\Delta e_s(k)$ along with the corresponding rule are summarized in Table 2.

As the outcome of rules R_{2a} and R_{2b} is the same, we merge these two rules into one using fuzzy OR operator, and the modified rule is called R_2 which is defined as follows:

R_2 : IF ($e_s(k)$ is E^{-1} AND $\Delta e_s(k)$ is ΔE^{+1}) OR ($e_s(k)$ is E^{+1} AND $\Delta e_s(k)$ is ΔE^{-1}) THEN $\Delta u_s(k)$ is ΔU^{0}.

To perform the AND operation in the rule base, AP and Min t-norms are used. Whereas for performing the OR operation in rule R_2, Max, BS and AS s-norms are utilized. For the basic definitions, properties and details of the t-norms and s-norms, one may refer to Klement et al. (2000). Note that the same rule base is also applicable for finding the analytical structures of the simplest fuzzy PD controllers provided

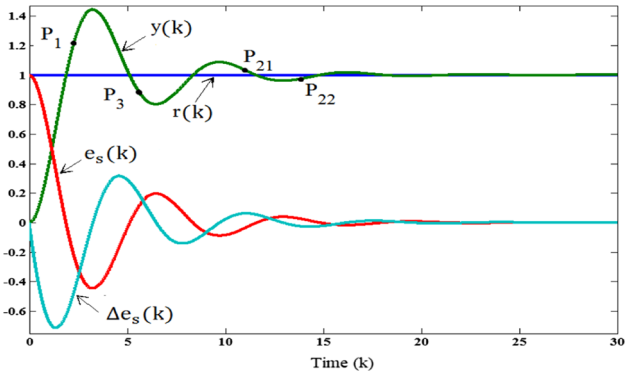

Fig. 5 Pictorial representation of rule base justification

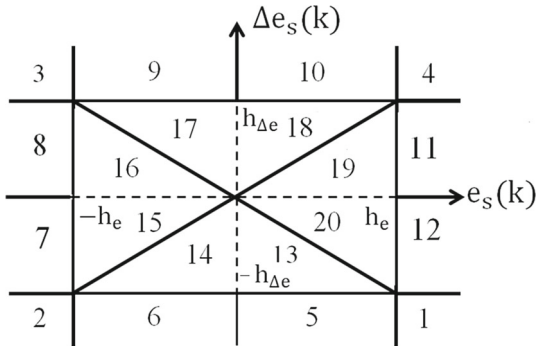

Fig. 6 Regions of scaled input plane

Table 2 Signs of $e_s(k)$ and $\Delta e_s(k)$ and corresponding rule under different cases

Case	$e_s(k)$	$\Delta e_s(k)$	Rule
1	Negative	Negative	R_1
2	Negative	Positive	R_{2a}
3	Positive	Negative	R_{2b}
4	Positive	Positive	R_3

$\Delta u_s(k)$ is replaced with $u_s(k)$ and ΔU^{-1}, ΔU^0 and ΔU^{+1} are replaced by U^{-1}, U^0 and U^{+1}, respectively.

All possible combinations of input variables, $e_s(k)$ and $\Delta e_s(k)$, are provided in Fig. 6 which can be obtained by looking downward along the μ axis and considering the top view of the 3D plot with axes $e_s(k)$, $\Delta e_s(k)$ and μ. In each region, the control rules $R_1 - R_3$ are exploited to obtain appropriate control effort. In Table 3 (using AP AND) and Table 4 (using Min AND), the resultant expressions (μ_{-1}, μ_0 and μ_{+1}) of the antecedent parts of all the three rules are provided.

3.3 Inference mechanism

By employing a particular type of inference mechanism, the outcomes of antecedent parts of the rules i.e. μ_{-1}, μ_0 and μ_{+1} are used to alter the reference output fuzzy sets ΔU^{-1} or U^{-1} (in rule R_1), ΔU^0 or U^0 (in rule R_2) and ΔU^{+1} or U^{+1} (in rule R_3), respectively. Throughout this study, LP inference mechanism is used. In Fig. 7, the modified membership functions obtained via LP inference method are shown with hatching.

3.4 Defuzzification

For the purpose of having a crisp value of the control effort, the set of modified control output values is converted by a process called defuzzification. In literature several defuzzification strategies are available. Among the various defuzzification strategies, from the control systems point of view, CoS is the most explored one. Though CoG method is more accurate as compared to the CoS method, because of its computational complexity it has not almost been explored and remained dormant for a long time for obtaining the analytical structures of the fuzzy controllers. Crisp value u^* through CoG method is formally given by:

$$u^* = \frac{\int_U u \cdot \max\limits_k \mu_U^{(k)}(u)\mathrm{d}u}{\int_U \max\limits_k \mu_U^{(k)}(u)\mathrm{d}u} \tag{6}$$

In a typical case the defuzzified value obtained via CoG and CoS defuzzification methods is graphically represented in Fig. 8. We observe that the defuzzified values are different when CoG and CoS defuzzification methods are used. Moreover, we notice that in CoS defuzzification the overlapping area of two adjacent regions is considered twice, while it is accounted only once in CoG defuzzification. This clearly indicates that the CoG defuzzification is more accurate than the CoS method. From the literature survey, it seems to the authors that till date, except Arun and Mohan (2017), no one has obtained the analytical structures of the simplest fuzzy PI/PD controllers using CoG defuzzification method. In Arun and Mohan (2017), analytical structures of only two classes of the simplest fuzzy PI/PD controllers (using AP t-norm, Max t-conorm and LP inference; and Min t-norm, Max t-conorm and Mamdani Minimum (MM) inference) have been obtained. In this paper, we reveal the exact analytical structures of another five classes of the simplest fuzzy PI/PD controllers using CoG defuzzification.

When the scaled inputs lie in regions 13-20 (except points $(-h_e, -h_{\Delta e})$ and $(h_e, h_{\Delta e})$), the aggregated control output (u_{ac}) corresponding to the LP inference is shown with shading in Fig. 9 where the membership grades of μ_{-1}, μ_0, and μ_{+1} are provided in Tables 3 and 4. From now onward we call regions 13-20 as inner regions. The crisp control output $u_s^*(k)$ of the fuzzy PD controller can be obtained from the

Table 3 Resultants of antecedent parts of control rules using t_{AP}, s_{BS}, and s_{AS}

Region	μ_{-1}	μ_0		μ_{+1}
		BS OR	AS OR	
1, 3	0	1	1	0
2	1	0	0	0
4	0	0	0	1
5, 6	$\mu_{E^{-1}}$	$\mu_{E^{+1}}$	$\mu_{E^{+1}}$	0
7, 8	$\mu_{\Delta E^{-1}}$	$\mu_{\Delta E^{+1}}$	$\mu_{\Delta E^{+1}}$	0
9, 10	0	$\mu_{E^{-1}}$	$\mu_{E^{-1}}$	$\mu_{E^{+1}}$
11, 12	0	$\mu_{\Delta E^{-1}}$	$\mu_{\Delta E^{-1}}$	$\mu_{\Delta E^{+1}}$
13-20	$\mu_{E^{-1}}.\mu_{\Delta E^{-1}}$	$\mu_{E^{-1}}.\mu_{\Delta E^{+1}} + \mu_{E^{+1}}.\mu_{\Delta E^{-1}}$	$\mu_{E^{-1}}.\mu_{\Delta E^{+1}} + \mu_{E^{+1}}.\mu_{\Delta E^{-1}} - \mu_{E^{-1}}.\mu_{\Delta E^{+1}}.\mu_{E^{+1}}.\mu_{\Delta E^{-1}}$	$\mu_{E^{+1}}.\mu_{\Delta E^{+1}}$

Table 4 Resultants of antecedent parts of control rules using t_{Min}, s_{BS}, s_{AS} and s_{Max}

Region	μ_{-1}	μ_0			μ_{+1}
		BS OR	AS OR	Max OR	
1 – 12		Same as provided in Table 3			
13, 14	$\mu_{E^{-1}}$	$\mu_{E^{+1}} + \mu_{\Delta E^{+1}}$	$\mu_{E^{+1}} + \mu_{\Delta E^{+1}} - \mu_{E^{+1}}.\mu_{\Delta E^{+1}}$	$\mu_{E^{+1}}$	$\mu_{\Delta E^{+1}}$
15, 16	$\mu_{\Delta E^{-1}}$	$\mu_{E^{+1}} + \mu_{\Delta E^{+1}}$	$\mu_{E^{+1}} + \mu_{\Delta E^{+1}} - \mu_{E^{+1}}.\mu_{\Delta E^{+1}}$	$\mu_{\Delta E^{+1}}$	$\mu_{E^{+1}}$
17, 18	$\mu_{\Delta E^{-1}}$	$\mu_{E^{-1}} + \mu_{\Delta E^{-1}}$	$\mu_{E^{-1}} + \mu_{\Delta E^{-1}} - \mu_{E^{-1}}.\mu_{\Delta E^{-1}}$	$\mu_{E^{-1}}$	$\mu_{E^{+1}}$
19, 20	$\mu_{E^{-1}}$	$\mu_{E^{-1}} + \mu_{\Delta E^{-1}}$	$\mu_{E^{-1}} + \mu_{\Delta E^{-1}} - \mu_{E^{-1}}.\mu_{\Delta E^{-1}}$	$\mu_{\Delta E^{-1}}$	$\mu_{\Delta E^{+1}}$

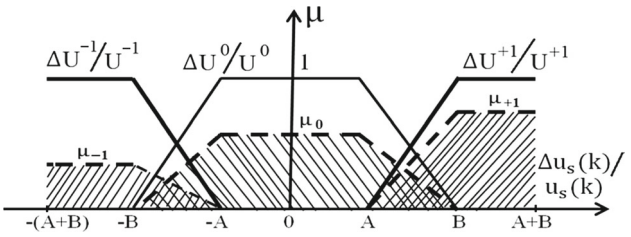

Fig. 7 Reference and inferred membership functions of the fuzzy sets on output variable ($\Delta u_s(k)$ or $u_s(k)$) via LP inference

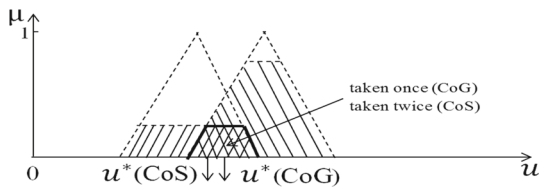

Fig. 8 Pictorial interpretation of CoG and CoS defuzzification strategies

shaded region as

$$u_s^*(k) = \frac{\int_{-(A+B)}^{A+B} \mu\, u_s\, \mathrm{d}u_s}{\int_{-(A+B)}^{A+B} \mu\, \mathrm{d}u_s} \tag{7}$$

We need to replace $u_s(k)$ by $\Delta u_s(k)$ in Eq. (7) for obtaining the crisp fuzzy PI controller output $\Delta u_s^*(k)$. When the

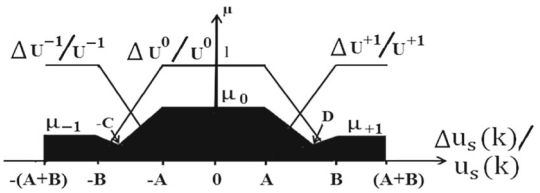

Fig. 9 u_{ac} via LP inference when $e_s(k)$ and $\Delta e_s(k)$ lie in inner regions

scaled inputs $e_s(k)$ and $\Delta e_s(k)$ lie in inner regions (except points $(-h_e, -h_{\Delta e})$ and $(h_e, h_{\Delta e})$), Eq. (7) can be calculated by referring to Fig. 9 and Eqs. (8) and (9).

$$\begin{aligned}\int_{-(A+B)}^{A+B} \mu\, u_s\, \mathrm{d}u_s = &\int_{-(A+B)}^{-B} \mu_{-1}\, u_s\, \mathrm{d}u_s + \int_{-B}^{-C} \mu_c\, u_s\, \mathrm{d}u_s \\ &+ \int_{-C}^{-A} \mu_a\, u_s\, \mathrm{d}u_s + \int_{-A}^{A} \mu_0\, u_s\, \mathrm{d}u_s + \int_{A}^{D} \mu_d\, u_s\, \mathrm{d}u_s \\ &+ \int_{D}^{B} \mu_b\, u_s\, \mathrm{d}u_s + \int_{B}^{A+B} \mu_{+1}\, u_s\, \mathrm{d}u_s \end{aligned} \tag{8}$$

and

$$\begin{aligned}\int_{-(A+B)}^{A+B} \mu\, \mathrm{d}u_s = &\int_{-(A+B)}^{-B} \mu_{-1}\, \mathrm{d}u_s + \int_{-B}^{-C} \mu_c\, \mathrm{d}u_s \\ &+ \int_{-C}^{-A} \mu_a\, \mathrm{d}u_s + \int_{-A}^{A} \mu_0\, \mathrm{d}u_s + \int_{A}^{D} \mu_d\, \mathrm{d}u_s \end{aligned}$$

Table 5 Analytical structures of proposed controllers (Classes 1–5) in regions 1–12 and at points P and Q

Region/point	Δu_s or u_s
1, 3	0
2,4	$\mp\frac{2(A^2+B^2)+5AB}{3(A+B)}$
5, 6, 9, 10	$\frac{[h_e^2(11A^2+20AB+5B^2)\pm 2e_s h_e(A^2+AB-2B^2)-e_s^2(B-A)^2](\mp h_e+e_s)}{6h_e[h_e^2(7A+5B)\pm 2e_s h_e(B+A)+e_s^2(B-A)]}$
7, 8, 11, 12	$\frac{[h_{\Delta e}^2(11A^2+20AB+5B^2)\pm 2\Delta e_s h_{\Delta e}(A^2+AB-2B^2)-\Delta e_s^2(B-A)^2](\mp h_{\Delta e}+\Delta e_s)}{6h_{\Delta e}[h_{\Delta e}^2(7A+5B)\pm 2\Delta e_s h_{\Delta e}(B+A)+\Delta e_s^2(B-A)]}$
P, Q	$\frac{2(A^2+B^2)+5AB}{6(A+B)h_e h_{\Delta e}}(\Delta e_s h_e + e_s h_{\Delta e})$

Upper sign is used for regions 2, 5–8, and lower sign is for regions 4, 9–12. At point P, $e_s = -h_e$ and $\Delta e_s = -h_{\Delta e}$ and at point Q, $e_s = h_e$ and $\Delta e_s = h_{\Delta e}$

Table 6 Analytical structure of Class 1 controller in inner regions except at points P and Q

Region	Δu_s or u_s
13–20	$\frac{\begin{array}{l} e_s^4\Delta e_s^4(-2A^2+25AB-14B^2)+2(\Delta e_s^2 h_e^2+e_s^2 h_{\Delta e}^2)[e_s^2\Delta e_s^2(-8A^2+AB-2B^2)+h_e h_{\Delta e}\{3h_e h_{\Delta e} \\ (-8A^2-13AB-6B^2)+4e_s\Delta e_s(7A^2+7AB+4B^2)\}](\Delta e_s^4 h_e^4+e_s^4 h_{\Delta e}^4)(2A^2+5AB+2B^2)+h_e \\ h_{\Delta e}[4e_s^2\Delta e_s^2\{3h_e h_{\Delta e}(24A^2+41AB-2B^2)+2e_s\Delta e_s(-7A^2-19AB+8B^2)\}+h_e^2 h_{\Delta e}^2\{4e_s\Delta e_s \\ (-110A^2-182AB-32B^2)+3h_e h_{\Delta e}(74A^2+131AB+38B^2)\}] \\ \hline 6(\Delta e_s^2 h_e^2+e_s^2 h_{\Delta e}^2)[e_s^2\Delta e_s^2\{e_s\Delta e_s(B+A)-h_e h_{\Delta e}(19A+3B)\}h_e^2 h_{\Delta e}^2\{e_s\Delta e_s(53A+13B)-3h_e h_{\Delta e} \\ (13A+5B)\}]+(\Delta e_s^4 h_e^4+e_s^4 h_{\Delta e}^4)\{3e_s\Delta e_s(-3A+B)+3h_e h_{\Delta e}(5A+B)\}+e_s^3\Delta e_s^3\{e_s^2\Delta e_s^2(3A-9B) \\ +h_e h_{\Delta e}\{3e_s\Delta e_s(A+37B)-4h_e h_{\Delta e}(81A+117B)\}\}+3h_e^3 h_{\Delta e}^3[e_s\Delta e_s\{4e_s\Delta e_s(109A+89B)-3h_e \\ h_{\Delta e}(205A+137B)\}]+27h_e^2 h_{\Delta e}^2(11A+7B) \end{array}}{}(\Delta e_s h_e + e_s h_{\Delta e})$

$$+\int_D^B \mu_b\, du_s + \int_B^{A+B} \mu_{+1}\, du_s \tag{9}$$

where $\mu_c = \frac{-\mu_{-1}(u_s+A)}{B-A}$, $\mu_a = \frac{\mu_0(u_s+B)}{B-A}$, $\mu_d = \frac{\mu_0(-u_s+B)}{B-A}$, $\mu_b = \frac{\mu_{+1}(u_s-A)}{B-A}$, $C = \frac{A\mu_{-1}+B\mu_0}{\mu_{-1}+\mu_0}$, and $D = \frac{B\mu_0+A\mu_{+1}}{\mu_0+\mu_{+1}}$.

Let us now discuss the reason behind excluding the points $(-h_e, -h_{\Delta e})$ and $(h_e, h_{\Delta e})$. $\int_{-(A+B)}^{A+B} \mu\, u_s\, du_s$ and $\int_{-(A+B)}^{A+B} \mu\, du_s$ exist only when all the integrals defined on the right hand side of Eq. (8) and Eq. (9) exist. For all the proposed controllers we notice that at points P $(-h_e, -h_{\Delta e})$ and Q $(h_e, h_{\Delta e})$, the values of μ_{-1}, μ_0, μ_{+1} are 1, 0, 0, and 0, 0, 1, respectively. In these two points the values of C and D have $\frac{0}{0}$ form and are undefined. Subsequently the integrations defined in Eq. (8) and Eq. (9) do not exist. The crisp control output $u_s^*(k)$ of the fuzzy PD controller at points P and Q can be obtained by referring to Eqs. (10) and (11), respectively.

$$u_s^*(k)|_P = \frac{\int_{-(A+B)}^{-B} u_s\, du_s + \int_{-B}^{-A} \mu_c|_{\mu_{-1}=1}\, u_s\, du_s}{\int_{-(A+B)}^{-B} du_s + \int_{-B}^{-A} \mu_c|_{\mu_{-1}=1}\, du_s} \tag{10}$$

$$u_s^*(k)|_Q = \frac{\int_A^B \mu_b|_{\mu_{+1}=1}\, u_s\, du_s + \int_B^{(A+B)} u_s\, du_s}{\int_A^B \mu_b|_{\mu_{+1}=1}\, du_s + \int_B^{(A+B)} du_s} \tag{11}$$

4 Mathematical models of the fuzzy PI/PD controllers

The input–output structural relationships of the simplest fuzzy PI or PD controllers (Class 1 to Class 5) are obtained and the scaled control output ($\Delta u_s(k)$ or $u_s(k)$) expressions are provided in Tables 5, 6, 7, 8, 9, 10. The control surfaces along with the gain plots of the proposed fuzzy controllers are depicted in Figs. 10, 11, 12, 13, 14, 15, 16, 17, 18 , 19 where the values of controller parameters are considered as: $A = 1, B = 2, h_e = 1, h_{\Delta e} = 1$ and for both the scaled inputs the UoD is [-2,2]. Note that for obtaining the gain plots of all the classes of controllers, the inner regions are only considered. From the controller structures, it is found that the proposed simplest fuzzy PI/PD controllers are different nonlinear PI/PD controllers with variable gains.

4.1 Properties of the proposed simplest fuzzy PI/PD controllers

The properties of the proposed simplest fuzzy PI/PD controllers are summarized below:

Table 7 Analytical structure of Class 2 controller in inner regions except at points P and Q

Region	Δu_s or u_s
13–20	$\frac{[12h_eh_{\Delta e}(A^2+2AB)\{e_s^2\Delta e_s^2\{e_s^2\Delta e_s^2\{e_s^2\Delta e_s^2\{e_s^2\Delta e_s^2-4(e_s^2h_{\Delta e}^2+\Delta e_s^2h_e^2)\}+6(e_s^4h_{\Delta e}^4+\Delta e_s^4h_e^4)\}-4(e_s^6h_{\Delta e}^6+\Delta e_s^6h_e^6)\}+(e_s^8h_{\Delta e}^8+\Delta e_s^8h_e^8)\}]+[96e_s\Delta e_sh_e^2h_{\Delta e}^2(2A^2+5AB-B^2)\{e_s^2\Delta e_s^2\{e_s^2\Delta e_s^2\{e_s^2\Delta e_s^2\{e_s^2\Delta e_s^2-3(e_s^2h_{\Delta e}^2+\Delta e_s^2h_e^2)\}+3(e_s^4h_{\Delta e}^4+\Delta e_s^4h_e^4)\}-(e_s^6h_{\Delta e}^6+\Delta e_s^6h_e^6)\}]-[8h_e^3h_{\Delta e}^3\{2(e_s^2h_{\Delta e}^2+\Delta e_s^2h_e^2)\{2e_s\Delta e_s\{e_s^2\Delta e_s^2\{e_s\Delta e_s(29A^2+185AB-97B^2)-h_eh_{\Delta e}(266A^2+281AB+155B^2)\}+h_e^2h_{\Delta e}^2\{h_eh_{\Delta e}(1234A^2+3085AB-521B^2)-e_s\Delta e_s(347A^2+1913AB-685B^2)\}\}-h_e^4h_{\Delta e}^4(1237A^2+2284AB-254B^2)\}-\{(e_s^4h_{\Delta e}^4+\Delta e_s^4h_e^4)\{4e_s\Delta e_s\{e_s\Delta e_s(10A^2+67AB-41B^2)-3h_eh_{\Delta e}(26A^2+129AB-29B^2)\}+h_e^2h_{\Delta e}^2(281A^21070AB-100B^2)\}+2(e_s^6h_{\Delta e}^6+\Delta e_s^6h_e^6)(5A^2+32AB-10B^2)\}\}]+[4h_e^3h_{\Delta e}^3\{4e_s\Delta e_s\{e_s^2\Delta e_s^2\{2e_s^2\Delta e_s^2\{3e_s\Delta e_s(6A^2+35AB-17B^2)-h_eh_{\Delta e}(170A^2-151AB+251B^2)\}-h_e^2h_{\Delta e}^2\{e_s\Delta e_s(1805A^2+1952AB-202B^2)-2h_eh_{\Delta e}(950A^2-313AB+2405B^2)\}\}+2h_e^4h_{\Delta e}^4\{e_s\Delta e_s(6194A^2+10193AB-1195B^2)-h_eh_{\Delta e}(10970A^2+18017AB+3683B^2)\}\}+11h_e^6h_{\Delta e}^6(3593A^2+6410AB+1976B^2)\}]}{(B+A)[-3e_s^2\Delta e_s^2\{e_s^2\Delta e_s^2\{e_s^2\Delta e_s^2\{e_s^2\Delta e_s^2\{e_s^2\Delta e_s^2-5(e_s^2h_{\Delta e}^2+\Delta e_s^2h_e^2)\}+10(e_s^4h_{\Delta e}^4+\Delta e_s^4h_e^4)\}-10(e_s^6h_{\Delta e}^6+\Delta e_s^6h_e^6)\}+5(e_s^8h_{\Delta e}^8+\Delta e_s^8h_e^8)\}+3(e_s^{10}h_{\Delta e}^{10}+\Delta e_s^{10}h_e^{10})]-24e_s\Delta e_sh_eh_{\Delta e}(3B+2A)[e_s^2\Delta e_s^2\{e_s^2\Delta e_s^2\{e_s^2\Delta e_s^2\{e_s^2\Delta e_s^2-4(e_s^2h_{\Delta e}^2+\Delta e_s^2h_e^2)\}+6(e_s^4h_{\Delta e}^4+\Delta e_s^4h_e^4)\}-4(e_s^6h_{\Delta e}^6+\Delta e_s^6h_e^6)\}+(e_s^8h_{\Delta e}^8+\Delta e_s^8h_e^8)]-3h_e^2h_{\Delta e}^2[e_s\Delta e_s\{e_s\Delta e_s\{e_s\Delta e_s\{e_s\Delta e_s\{e_s\Delta e_s\{e_s\Delta e_s\{e_s\Delta e_s\{e_s\Delta e_s(209B+41A)+128h_eh_{\Delta e}(4B-5A)\}-12h_e^2h_{\Delta e}^2(205B+301A)\}-32h_e^3h_{\Delta e}^3(321B-182A)\}+20h_e^4h_{\Delta e}^4(1181B+2709A)\}+128h_e^5h_{\Delta e}^5(364B-333A)\}-h_e^6h_{\Delta e}^6(230375B+275559A)\}+88h_e^7h_{\Delta e}^7(3353B+5238A)\}-1331h_e^8h_{\Delta e}^8(93B+149A)]+3h_e^2h_{\Delta e}^2(e_s^2h_{\Delta e}^2+\Delta e_s^2h_e^2)[2e_s\Delta e_s\{e_s\Delta e_s\{e_s\Delta e_s\{e_s\Delta e_s\{e_s\Delta e_s\{e_s\Delta e_s\{e_s\Delta e_s(281B+41A)-32h_eh_{\Delta e}(B+28A)\}-2h_e^2h_{\Delta e}^2(2023B+1271A)\}+32h_e^3h_{\Delta e}^3(11B+208A)\}+h_e^4h_{\Delta e}^4(29529B+11705A)\}-16h_e^5h_{\Delta e}^5(2705B+1974A)\}+11h_e^6h_{\Delta e}^6(3055B+2511A)]-6h_e^2h_{\Delta e}^2(e_s^4h_{\Delta e}^4+\Delta e_s^4h_e^4)[e_s\Delta e_s\{e_s\Delta e_s\{e_s\Delta e_s\{e_s\Delta e_s(241B+25A)-64h_eh_{\Delta e}(10B+11A)\}-h_e^2h_{\Delta e}^2(2279B+551A)\}+8h_e^3h_{\Delta e}^3(673B+350A)\}-h_e^4h_{\Delta e}^4(2947B+1563A)]+3h_e^2h_{\Delta e}^2(e_s^6h_{\Delta e}^6+\Delta e_s^6h_e^6)[2h_e^2h_{\Delta e}^2(261B+149A)+e_s\Delta e_s\{e_s\Delta e_s(89B-7A)-160h_eh_{\Delta e}(5B+2A)\}]+3h_e^2h_{\Delta e}^2(e_s^8h_{\Delta e}^8+\Delta e_s^8h_e^8)(35B+11A)}$ $(\Delta e_sh_e+e_sh_{\Delta e})$

Table 8 Analytical structure of Class 3 controller in inner regions except at points P and Q

Region	Δu_s or u_s
13, 14, 17, 18	$\frac{\Delta e_s^2h_e^2\{\Delta e_sh_e\{\{\Delta e_sh_e(11A^2+20AB+5B^2)+e_sh_{\Delta e}(13A^2+25AB-2B^2)\}\pm3h_eh_{\Delta e}(33A^2+59AB+16B^2)\}\pm h_{\Delta e}^2\{e_s\{\pm e_s(2A^2+17AB-10B^2)+9h_e(11A^2+19AB)\}\pm3h_e^2(107A^2+190AB+54B^2)\}\}-h_{\Delta e}^3\{\Delta e_sh_e\{e_s\{3e_s\{e_s(A^2-3AB+2B^2)\mp h_e(7A^2+23AB-12B^2)\}-3h_e^2(78A^2+130AB+8B^2)\}\mp6h_e^3(74A^2+131AB+38B^2)\}+h_{\Delta e}\{e_s^3\{e_s(B-A)^2\pm3h_e(A^2-5AB+4B^2)\}-h_e^2\{\pm e_s\{\pm3e_s(11A^2+26AB-10B^2)+2h_e(86A^2+143AB+14B^2)\}+3h_e^2(74A^2+131AB+38B^2)\}\}\}}{\pm3h_e\{\Delta e_s^2h_e\{\Delta e_sh_e^2\{\Delta e_s\{2\Delta e_sh_e(5B+7A)+e_sh_{\Delta e}(17B+15A)\}\pm h_{\Delta e}\{\Delta e_sh_e(107B+157A)+4e_sh_{\Delta e}(37B+38A)\}\}+2h_{\Delta e}^2\{\Delta e_sh_e\{9h_e^2(25B+38A)+7Be_s^2\}+h_{\Delta e}\{e_s^2\{e_s(3B-2A)\pm2h_e(23B+4A)\}+h_e^2\{e_s(238B+275A)\pm3h_e(155B+241A)\}\}\}\}+h_{\Delta e}^4\{e_s\{\pm e_s^2\{\pm e_s(B-A)(\Delta e_s\pm3h_{\Delta e})+4\Delta e_sh_e(7B-4A)\}+2\Delta e_sh_e^2\{e_s(98B+37A)\pm84h_e(4B+5A)\}\}+h_e\{2e_s^2h_{\Delta e}\{3e_s(5B-2A)\pm3h_e(23B+13A)\}+27h_e^2\{e_sh_{\Delta e}(13B+17A)+(7B+11A)(5\Delta e_sh_e\pm2h_eh_{\Delta e})\}\}\}}$ $(\Delta e_sh_e+e_sh_{\Delta e})$
15, 16, 19, 20	$\frac{e_s^2h_{\Delta e}^2\{e_sh_{\Delta e}\{\{e_sh_{\Delta e}(11A^2+20AB+5B^2)+\Delta e_sh_e(13A^2+25AB-2B^2)\}\pm3h_eh_{\Delta e}(33A^2+59AB+16B^2)\}\pm h_e^2\{\Delta e_s\{\pm\Delta e_s(2A^2+17AB-10B^2)+9h_{\Delta e}(11A^2+19AB)\}\pm3h_{\Delta e}^2(107A^2+190AB+54B^2)\}\}-h_e^3\{e_sh_{\Delta e}\{\Delta e_s\{3\Delta e_s\{\Delta e_s(A^2-3AB+2B^2)\mp h_{e\Delta}(7A^2+23AB-12B^2)\}-3h_{\Delta e}^2(78A^2+130AB+8B^2)\}\mp6h_{\Delta e}^3(74A^2+131AB+38B^2)\}+h_e\{\Delta e_s^3\{\Delta e_s(B-A)^2\pm3h_{\Delta e}(A^2-5AB+4B^2)\}-h_{\Delta e}^2\{\pm\Delta e_s\{\pm3\Delta e_s(11A^2+26AB-10B^2)+2h_{\Delta e}(86A^2+143AB+14B^2)\}+3h_{\Delta e}^2(74A^2+131AB+38B^2)\}\}\}}{\pm3h_{\Delta e}\{e_s^2h_{\Delta e}\{e_sh_e^2\{e_s\{2e_sh_{\Delta e}(5B+7A)+\Delta e_sh_e(17B+15A)\}\pm h_e\{e_sh_{\Delta e}(107B+157A)+4\Delta e_sh_e(37B+38A)\}\}+2h_e^2\{e_sh_{\Delta e}\{9h_{\Delta e}^2(25B+38A)+7B\Delta e_s^2\}+h_e\{\Delta e_s^2\{\Delta e_s(3B-2A)\pm2h_{\Delta e}(23B+4A)\}+h_{\Delta e}^2\{\Delta e_s(238B+275A)\pm3h_{\Delta e}(155B+241A)\}\}\}+h_e^4\{\Delta e_s\{\pm\Delta e_s^2\{\pm\Delta e_s(B-A)(e_s\pm3h_e)+4e_sh_{\Delta e}(7B-4A)\}+2e_sh_{\Delta e}^2\{\Delta e_s(98B+37A)\pm84h_{\Delta e}(4B+5A)\}\}+h_{\Delta e}\{2\Delta e_s^2h_e\{3\Delta e_s(5B-2A)\pm3h_{\Delta e}(23B+13A)\}+27h_{\Delta e}^2\{\Delta e_sh_e(13B+17A)+(7B+11A)(5e_sh_{\Delta e}\pm2h_eh_{\Delta e})\}\}\}}$ $(\Delta e_sh_e+e_sh_{\Delta e})$

Upper sign and lower sign are used for regions 13-16 and 17-20, respectively, in Tables 8-10

Table 9 Analytical structure of Class 4 controller in inner regions except at points P and Q

Region	Δu_s or u_s
13, 14, 17, 18	$\{\Delta e_s\{\Delta e_s\{\Delta e_s\{\Delta e_s\{e_s\{e_s\{3\ e_s\{e_s(A^2+2AB)\mp 2h_e(4A^2+7AB+B^2)\}+2h_e^2(31A^2+55AB+13B^2)\}\mp 2h_e^3(32A^2+59AB+17B^2)\}+h_e^4(23A^2+44AB+14B^2)\}+2h_{\Delta e}\{e_s\{e_s\{e_s\{\pm 3e_s(B^2-AB)-2h_e(17A^2+26AB+11B^2)\}\pm 2h_e^2(95A^2+161AB+50B^2)\}-2h_e^3(155A^2+278AB+89B^2)\}\pm h_e^4(154A^2+289AB+97B^2)\}\}-2h_{\Delta e}^2\{e_s\{e_s\{e_s\{e_s(5A^2-AB+5B^2)\mp 2h_e(13A^2+13AB-8B^2)\}-2h_e^2(112A^2+214AB+97B^2)\}\pm 10h_e^3(89A^2+161AB+56B^2)\}-h_e^4(709A^2+1315AB+451B^2)\}\}\pm 2h_{\Delta e}^3\{e_s\{e_s\{e_s\{e_s(4A^2-5AB+B^2)\pm 2h_e(17A^2+14AB+23B^2)\}-2h_e^2(59A^2+53AB-22B^2)\}\mp 6h_e^3(119A^2+234AB+97B^2)\}+h_e^4(1306A^2+2383AB+811B^2)\}\}+h_{\Delta e}^4\{e_s\{e_s\{e_s\{e_s(-A^2+8AB+2B^2)\mp 2h_e(14A^2-19AB+5B^2)\}-2h_e^2(71A^2+59AB+95B^2)\}\pm 90h_e^3(2A^2+AB-3B^2)\}+5h_e^4(331A^2+598AB+196B^2)\}\}$ $-3\Delta e_s\{\Delta e_s\{\Delta e_s\{\Delta e_s\{\Delta e_s\{e_s\{e_s\{e_s\{e_s\{e_s(B+A)\mp h_e(9B+11A)\}+4h_e^2(8B+11A)\}\mp 8h_e^3(7B+10A)\}+h_e^4(47B+67A)\}\mp h_e^5(15B+21A)\}-h_eh_{\Delta e}\{e_s\{e_s\{e_s\{e_s(19B+39A)\mp 56h_e(3B+5A)\}+4h_e^2(118B+189A)\}\mp h_e^3(553B+855A)\}+h_e^4(229B+341A)\}\}-4e_sh_{\Delta e}^2\{e_s\{e_s\{e_s\{Ae_s\mp 2h_e(2B+A)\}-h_e^2(45B+101A)\}\pm h_e^3(313B+555A)\}-h_e^4(579B+956A)\}\}\mp 4h_eh_{\Delta e}^2\{\{\{\{\Delta e_sh_e^4(331B+519A)\mp 17Ae_s^4h_{\Delta e}\}+e_s^3h_eh_{\Delta e}(21B+43A)\}\pm e_s^2h_e^2h_{\Delta e}(247B+483A)\}-7e_sh_e^3h_{\Delta e}(147B+253A)\}\pm 5h_e^4h_{\Delta e}(181B+294A)\}\}-h_{\Delta e}^4\{e_s\{e_s\{e_s\{e_s\{e_s(B-3A)\mp h_e(9B-13A)\}+20h_e^2(B+16A)\}\mp 4h_e^3(47B+103A)\}-5h_e^4(513B+937A)\}\pm 25h_e^5(189B+311A)\}\}\pm 3h_{\Delta e}\{e_s(B-A)\{e_s^2\{e_s^2(\Delta e_s^4-h_{\Delta e}^4)+20h_e^2h_{\Delta e}^4\}+125h_e^4h_{\Delta e}^4\}\mp h_{\Delta e}^4\{e_s^2h_e\{e_s^2(3B-13A)+20h_e^2(B+24A)\}-125h_e^5(19B+31A)\}\}$ $(\Delta e_sh_e+e_sh_{\Delta e})$
15, 16, 19, 20	$\{e_s\{e_s\{e_s\{e_s\{\Delta e_s\{\Delta e_s\{3\ \Delta e_s\{\Delta e_s(A^2+2AB)\mp 2h_{\Delta e}(4A^2+7AB+B^2)\}+2h_{\Delta e}^2(31A^2+55AB+13B^2)\}\mp 2h_{\Delta e}^3(32A^2+59AB+17B^2)\}+h_{\Delta e}^4(23A^2+44AB+14B^2)\}+2h_e\{\Delta e_s\{\Delta e_s\{\Delta e_s\{\pm 3\Delta e_s(B^2-AB)-2h_{\Delta e}(17A^2+26AB+11B^2)\}\pm 2h_{\Delta e}^2(95A^2+161AB+50B^2)\}-2h_{\Delta e}^3(155A^2+278AB+89B^2)\}\pm h_{\Delta e}^4(154A^2+289AB+97B^2)\}\}-2h_e^2\{\Delta e_s\{\Delta e_s\{\Delta e_s\{\Delta e_s(5A^2-AB+5B^2)\mp 2h_{\Delta e}(13A^2+13AB-8B^2)\}-2h_{\Delta e}^2(112A^2+214AB+97B^2)\}\pm 10h_{\Delta e}^3(89A^2+161AB+56B^2)\}-h_{\Delta e}^4(709A^2+1315AB+451B^2)\}\}\pm 2h_e^3\{\Delta e_s\{\Delta e_s\{\Delta e_s\{\Delta e_s(4A^2-5AB+B^2)\pm 2h_{\Delta e}(17A^2+14AB+23B^2)\}-2h_{\Delta e}^2(59A^2+53AB-22B^2)\}\mp 6h_{\Delta e}^3(119A^2+234AB+97B^2)\}+h_{\Delta e}^4(1306A^2+2383AB+811B^2)\}\}+h_e^4\{\Delta e_s\{\Delta e_s\{\Delta e_s\{\Delta e_s(-A^2+8AB+2B^2)\mp 2h_{\Delta e}(14A^2-19AB+5B^2)\}-2h_{\Delta e}^2(71A^2+59AB+95B^2)\}\pm 90h_{\Delta e}^3(2A^2+AB-3B^2)\}+5h_{\Delta e}^4(331A^2+598AB+196B^2)\}\}$ $-3e_s\{e_s\{e_s\{e_s\{e_s\{\Delta e_s\{\Delta e_s\{\Delta e_s\{\Delta e_s\{\Delta e_s(B+A)\mp h_{\Delta e}(9B+11A)\}+4h_{\Delta e}^2(8B+11A)\}\mp 8h_{\Delta e}^3(7B+10A)\}+h_{\Delta e}^4(47B+67A)\}\mp h_{\Delta e}^5(15B+21A)\}-h_{\Delta e}h_e\{\Delta e_s\{\Delta e_s\{\Delta e_s\{\Delta e_s(19B+39A)\mp 56h_{\Delta e}(3B+5A)\}+4h_{\Delta e}^2(118B+189A)\}\mp h_{\Delta e}^3(553B+855A)\}+h_{\Delta e}^4(229B+341A)\}\}-4\Delta e_sh_e^2\{\Delta e_s\{\Delta e_s\{\Delta e_s\{A\Delta e_s\mp 2h_{\Delta e}(2B+A)\}-h_{\Delta e}^2(45B+101A)\}\pm h_{\Delta e}^3(313B+555A)\}-h_{\Delta e}^4(579B+956A)\}\}\mp 4h_{\Delta e}h_e^2\{\{\{\{e_sh_{\Delta e}^4(331B+519A)\mp 17A\Delta e_s^4h_e\}+\Delta e_s^3h_{\Delta e}h_e(21B+43A)\}\pm\Delta e_s^2h_{\Delta e}^2h_e(247B+483A)\}-7\Delta e_sh_{\Delta e}^3h_e(147B+253A)\}\pm 5h_{\Delta e}^4h_e(181B+294A)\}\}-h_e^4\{\Delta e_s\{\Delta e_s\{\Delta e_s\{\Delta e_s\{\Delta e_s(B-3A)\mp h_{\Delta e}(9B-13A)\}+20h_{\Delta e}^2(B+16A)\}\mp 4h_{\Delta e}^3(47B+103A)\}-5h_{\Delta e}^4(513B+937A)\}\pm 25h_{\Delta e}^5(189B+311A)\}\}\pm 3h_e\{\Delta e_s(B-A)\{\Delta e_s^2\{\Delta e_s^2(e_s^4-h_e^4)+20h_{\Delta e}^2h_e^4\}+125h_{\Delta e}^4h_e^4\}\mp h_e^4\{\Delta e_s^2h_{\Delta e}\{\Delta e_s^2(3B-13A)+20h_{\Delta e}^2(B+24A)\}-125h_{\Delta e}^5(19B+31A)\}\}$ $(\Delta e_sh_e+e_sh_{\Delta e})$

Table 10 Analytical structure of Class 5 controller in inner regions except at points P and Q

Region	Δu_s or u_s
13, 14, 17, 18	$4\Delta e_s^2h_e^4(2A^2+5AB+2B^2)-e_s^2h_{\Delta e}\{\{e_s(\Delta e_sh_e+e_sh_{\Delta e})(B-A)^2\pm 3\Delta e_sh_e^2(B^2-A^2)\}+h_eh_{\Delta e}\{\pm e_s(A^2-8AB+7B^2)-h_e(17A^2+26AB-7B^2)\}\}+h_e^3h_{\Delta e}\{\Delta e_s\{e_s(25A^2+34AB+13B^2)\pm h_e(37A^2+76AB+31B^2)\}\pm h_{\Delta e}\{e_s(49A^2+76AB+19B^2)\pm h_e(40A^2+76AB+28B^2)\}\}$ $\pm 6h_e^2\{2\Delta e_s^3h_e^3(B+A)\pm h_{\Delta e}\{\Delta e_sh_e\{\Delta e_sh_e\{\pm 4e_s(B+2A)+h_e(13B+19A)\}\pm 2e_sh_{\Delta e}\{2e_s(2B+A)\pm h_e(11B+21A)\}\}\pm e_s^2h_{\Delta e}^2\{2e_s(3B-A)\pm h_e(17B+15A)\}\}\}+\{6e_s^2h_eh_{\Delta e}\{e_s^2h_{\Delta e}^2+\Delta e_sh_e(\Delta e_sh_e+2e_sh_{\Delta e})\}\}(B-A)\pm\{12h_e^4h_{\Delta e}^2\{5(\Delta e_sh_e+e_sh_{\Delta e})\pm 4h_eh_{\Delta e}\}\}(3B+5A)$ $(\Delta e_sh_e+e_sh_{\Delta e})$
15, 16, 19, 20	$4e_s^2h_{\Delta e}^4(2A^2+5AB+2B^2)-\Delta e_s^2h_e\{\{\Delta e_s(\Delta e_sh_e+e_sh_{\Delta e})(B-A)^2+3e_sh_{\Delta e}^2(B^2-A^2)\}+h_eh_{\Delta e}\{\pm\Delta e_s(A^2-8AB+7B^2)-h_{\Delta e}(17A^2+26AB-7B^2)\}\}+h_eh_{\Delta e}^3\{e_s\{\Delta e_s(25A^2+34AB+13B^2)\pm h_{\Delta e}(37A^2+76AB+31B^2)\}\pm h_e\{\Delta e_s(49A^2+76AB+19B^2)\pm h_{\Delta e}(40A^2+76AB+28B^2)\}\}$ $\pm 6h_{\Delta e}^2\{2e_s^3h_{\Delta e}^3(B+A)\pm h_e\{e_sh_{\Delta e}\{e_sh_{\Delta e}\{\pm 4\Delta e_s(B+2A)+h_{\Delta e}(13B+19A)\}\pm 2\Delta e_sh_e\{2\Delta e_s(2B+A)\pm h_{\Delta e}(11B+21A)\}\}\pm\Delta e_s^2h_e^2\{2\Delta e_s(3B-A)\pm h_{\Delta e}(17B+15A)\}\}\}+\{6\Delta e_s^2h_eh_{\Delta e}\{\Delta e_s^2h_e^2+e_sh_{\Delta e}(e_sh_{\Delta e}+2\Delta e_sh_e)\}\}(B-A)\pm\{12h_e^2h_{\Delta e}^4\{5(\Delta e_sh_e+e_sh_{\Delta e})\pm 4h_eh_{\Delta e}\}\}(3B+5A)$ $(\Delta e_sh_e+e_sh_{\Delta e})$

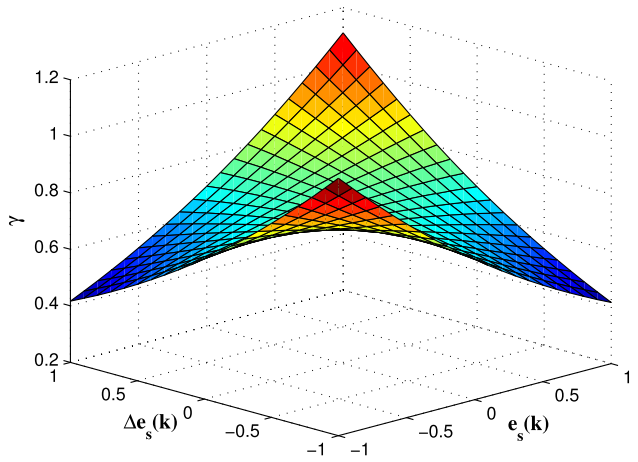

Fig. 10 Gain of the Class 1 controller

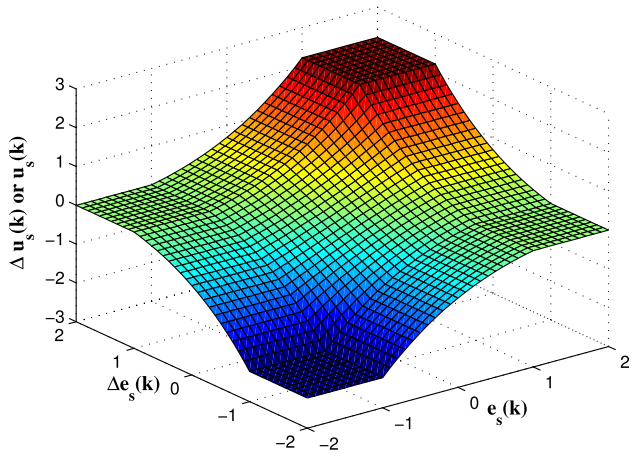

Fig. 11 Scaled control output (Class 1)

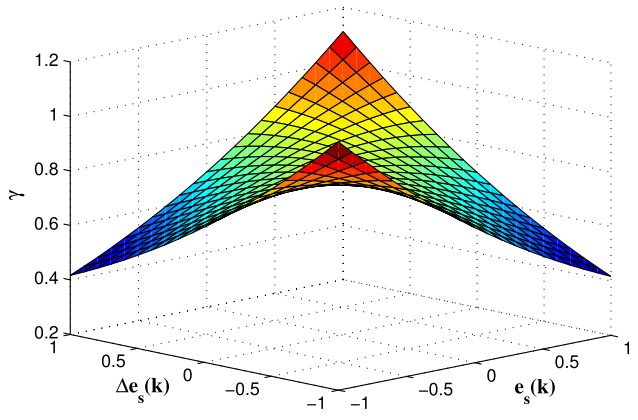

Fig. 12 Gain of the Class 2 controller

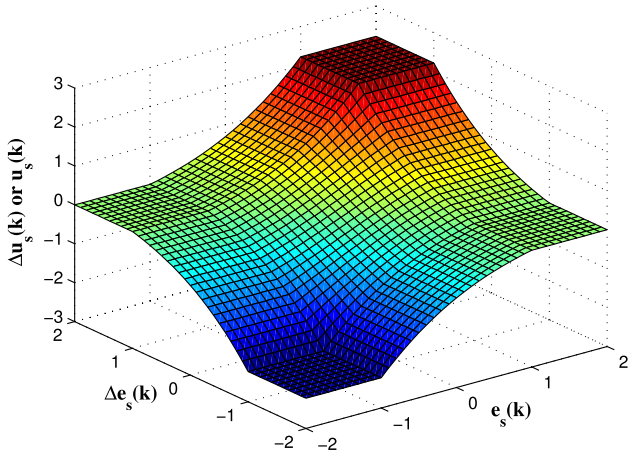

Fig. 13 Scaled control output (Class 2)

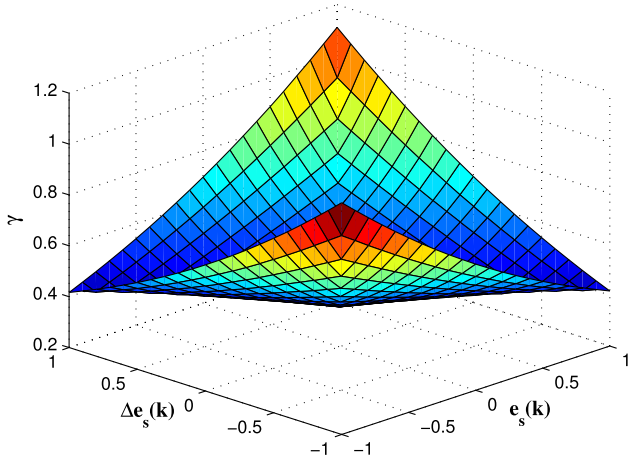

Fig. 14 Gain of the Class 3 controller

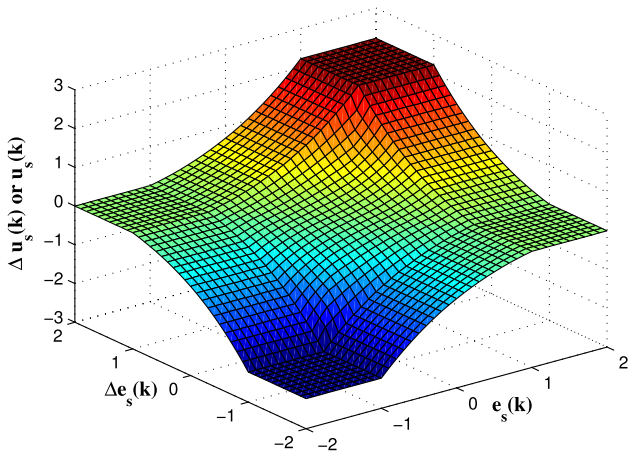

Fig. 15 Scaled control output (Class 3)

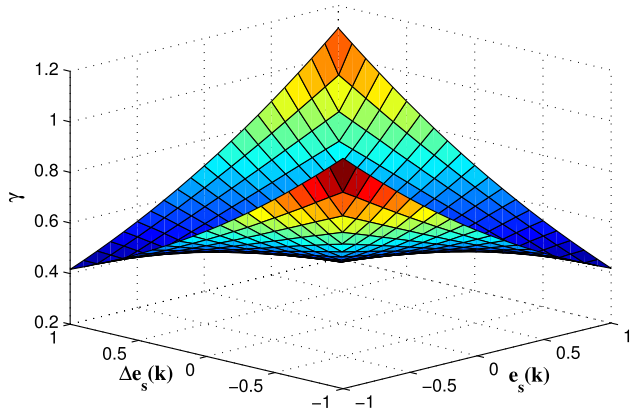

Fig. 16 Gain of the Class 4 controller

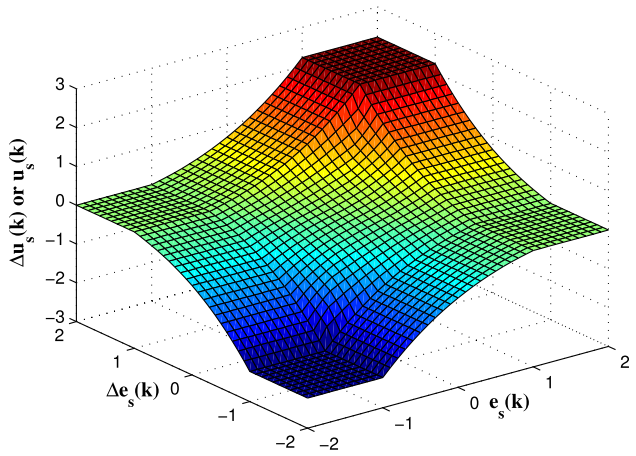

Fig. 17 Scaled control output (Class 4)

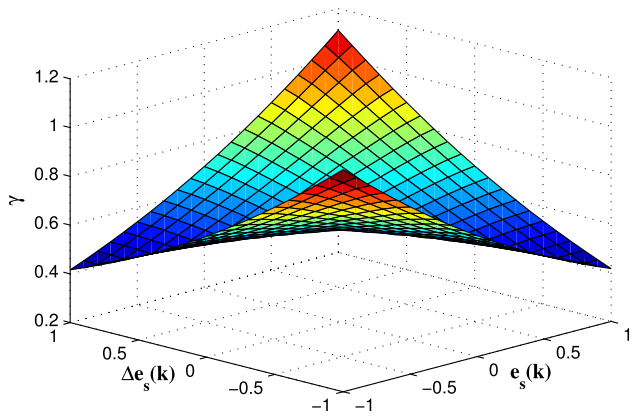

Fig. 18 Gain of the Class 5 controller

1. All the controllers are nonlinear and variable structure in nature.
2. They are variable gain controllers as the gain of each controller is a nonlinear function of the scaled input $e_s(k)$ or $\Delta e_s(k)$ or both. For all the classes of controllers, the scaled control output $\Delta u_s(k)$ or $u_s(k)$ in the inner regions can be written as $\Delta u_s(k)$ or $u_s(k) = \gamma(\Delta e_s(k)h_e + e_s(k)h_{\Delta e})$. This indicates that as in linear PI/PD controllers, the gains associated with $e_s(k)$ and $\Delta e_s(k)$ of the simplest fuzzy PI/PD controllers are different.
3. The minimum control effort produced by the controllers is $\frac{-[2(A^2+B^2)+5AB]}{3(A+B)}$ and it occurs at point P.
4. The maximum control effort produced by the controllers is $\frac{[2(A^2+B^2)+5AB]}{3(A+B)}$ and it occurs at point Q.
5. Control effort of the controllers is zero at $(e_s(k), \Delta e_s(k)) = (0, 0)$ and along the line $\Delta e_s(k) = -\frac{h_{\Delta e}}{h_e} e_s(k)$.
6. The control effort is continuous. When $h_e = h_{\Delta e}$, control effort is symmetric about the line $\Delta e_s(k) = \frac{h_{\Delta e}}{h_e} e_s(k)$.
7. The magnitude of control effort increases monotonically from the minimum value to the maximum value.

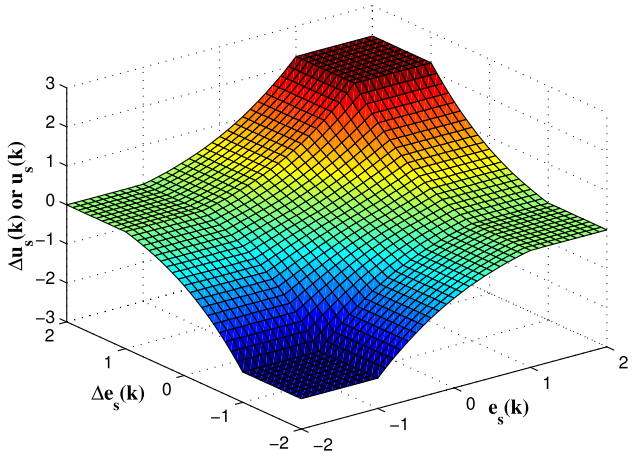

Fig. 19 Scaled control output (Class 5)

5 BIBO stability analysis

Ensuring stability is one of the most important aspects of control systems engineering. Several approaches have emerged over time to analyze the stability of a feedback control system. Small-Gain theorem (Khalil 2015) is one of them. In this section, with the help of Small-Gain theorem the sufficient conditions for BIBO stability of a feedback control system containing one of the proposed fuzzy PI controllers in the loop are established. For analyzing the stability, let us consider a feedback system depicted in Fig. 20. The gains of two systems G_1 and G_2 are considered as Ψ_1 and Ψ_2, respectively. As per the Small-Gain theorem, in response to any bounded input pair u_1 and u_2, a bounded output pair y_1 and y_2 is produced only when the product of system gains Ψ_1 and Ψ_2 is less than unity i.e. $\Psi_1\Psi_2 < 1$.

Now by defining $u_1(k) = r(k)$, $e_1(k) = e(k)$, $y_1(k) = \Delta u(k) = G_1 e_1(k)$, $u_2(k) = u(k-1)$, $e_2(k) = u(k)$ and $y_2(k) = y(k) = G_2 e_2(k)$ in Fig. 20, we get an equivalent representation of the closed loop system depicted in Fig. 1

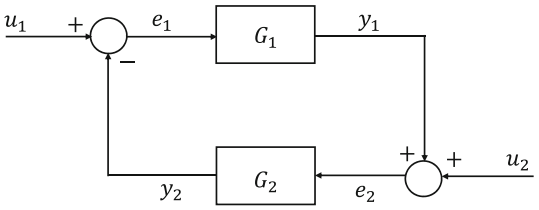

Fig. 20 A feedback system

where the digital controller is assumed to be a fuzzy PI controller. Under this set up, G_1 and G_2 become the controller and plant, respectively. We consider a general case where the plant under consideration is nonlinear and assume that the signal u_2 is bounded.

Let $N_e = \sup_{k\geq 0} |e(k)|$; $S_e \cdot N_e = h_e$ and $N_{\Delta e} = \sup_{k\geq 0} |\Delta e(k)| = \sup_{k\geq 0} |e(k) - e(k-1)| \leq 2N_e$; $S_{\Delta e} \cdot N_{\Delta e} = h_{\Delta e}$.

In the inner regions, from the analytical structures of the proposed fuzzy PI controllers it can be shown that

$$\|\Delta u(k)\| \leq \frac{[2(A^2 + B^2) + 5AB](h_e + h_{\Delta e})}{6(A + B)S_{\mathrm{PI}} h_e h_{\Delta e}} \|e_1(k)\| + \text{constant, for Classes 1 to 5.}$$

From the above inequality, the value of Ψ_1 is found to be

$$\Psi_1 = \frac{[2(A^2 + B^2) + 5AB](h_e + h_{\Delta e})}{6(A + B)S_{\mathrm{PI}} h_e h_{\Delta e}}, \quad \text{for Classes } 1 - 5. \tag{12}$$

Now for a finite gain L_∞ stable nonlinear system, we have

$$\|y_2(k)\| = \|G_2 e_2(k)\| \leq \|N\| \|e_2(k)\| \text{ so that}$$
$$\Psi_2 = \|N\| \tag{13}$$

From the analytical structures of the proposed controllers we observe that in regions 1 and 3, $\|\Delta u(k)\| = 0$ and therefore $\Psi_1 = 0$. To ensure $\Psi_1 \Psi_2 < 1$, it is sufficient to have $\Psi_2 < \infty$, and it is natural as the nonlinear system under consideration is finite gain L_∞ stable. Based on the previous discussions, the sufficient conditions for the nonlinear fuzzy PI feedback control system to be BIBO stable are:

1. The nonlinear process under consideration has a bounded norm and
2. The parameters $A, B, h_e, h_{\Delta e}$, and S_{PI} of the fuzzy PI controller should satisfy the inequality $\frac{[2(A^2+B^2)+5AB](h_e+h_{\Delta e})}{6(A+B)S_{\mathrm{PI}} h_e h_{\Delta e}} \|N\| < 1$.

By replacing S_{PI} by S_{PD} in the above inequality and considering $y_1(k) = u(k)$ and $u_2(k) = 0$, the conditions for the BIBO stability of nonlinear fuzzy PD feedback control system can also be obtained and stated as follows:

1. The nonlinear process under consideration has a bounded norm and
2. The parameters $A, B, h_e, h_{\Delta e}$, and S_{PD} of the fuzzy PD controller should satisfy the inequality $\frac{[2(A^2+B^2)+5AB](h_e+h_{\Delta e})}{6(A+B)S_{\mathrm{PD}} h_e h_{\Delta e}} \|N\| < 1$.

These stability conditions can be used as additional constraints during the design of proposed controllers, and the parameters obtained via these constraints will ensure the BIBO stability of the closed loop control system. But as finding the L_∞ norm of any arbitrary nonlinear dynamical system itself is a real challenging problem, in this study the stability results are not utilized in the numerical examples. This should not be viewed as the drawback of the proposed controllers.

Table 11 Computational aspects of fuzzy and linear PI/PD controllers (Class 1 - Class 5)

Controller class	1	2	3	4	5	Linear PI / PD
On-line operations	113	490	106	149	75	1
Off-line operations	104	251	169	280	83	0
Memory locations	34	73	51	82	34	0

6 Computational aspects of fuzzy PI/PD controllers

From the implementation point of view, it is of extreme importance to know the computational aspects of the controllers as the computational delay directly depends on it and affects the system performance. In spite of its importance, from literature it seems that not much work has been reported on the computational aspects of fuzzy PI/PD controllers. For different classes of controllers the required number of mathematical operations and memory locations have been calculated. The findings are summarized in Table 11 and graphically represented in Fig. 21. By on-line operations we mean those operations which need to be performed at every sampling instant. Whereas the off-line operations are performed once, stored and utilized as and when required. The mathematical operations which are common for both linear and fuzzy controllers are neglected as our target is to find additional computational burden incurred by the fuzzy PI/PD controllers. From Table 11, we notice that among the controllers that we have discussed, linear PI/PD controllers are the most attractive ones. But we should also understand that the additional computational burden encountered by the proposed fuzzy PI/PD controllers can easily be handled by high

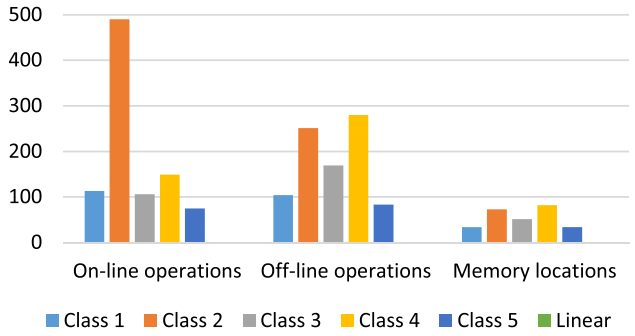

Fig. 21 Computational aspects of different controllers

Table 12 Optimized fuzzy PI controller parameters (Class 1–Class 5, Example 1)

Parameter	Class 1	Class 2	Class 3	Class 4	Class 5
A	0	0	0	0	0
B	0.0075	0.0099	0.0100	0.0100	0.0099
h_e	58.5161	58.3060	58.6579	58.0450	58.2082
$h_{\Delta e}$	0.9803	0.9803	1.0071	0.9802	1.0098
S_e	0.2759	0.2971	0.3087	0.2791	0.3078
$S_{\Delta e}$	7.3900	9.9707	7.0000	9.9736	7.0029
S_{PI}^{-1}	8.0039	9.9844	9.9257	9.9804	9.9629

Note: During optimization, the lower and upper bounds of the parameters B, h_e, $h_{\Delta e}$, S_e, $S_{\Delta e}$, and S_{PI}^{-1} are considered as $0.0075 - 0.01$, $58 - 59$, $0.98 - 1.01$, $0.275 - 0.31$, $7 - 10$, and $8 - 10$, respectively

speed computers. For efficient control, an important issue is to maintain the calculation time of a controller expression less than the sampling time T, and we have followed this particular constraint in simulation and real-time studies discussed in Sects. 7 and 8.

7 Simulation study

In this section, we consider two examples and demonstrate the applicability of proposed simplest fuzzy PI/PD controllers. For comparison purpose, both the examples are considered from Mudi and Pal (1999). The cost function considered in this study is as follows:

$$J = \frac{T}{T_{\mathrm{f}}} \sum_{k=0}^{\frac{T_{\mathrm{f}}}{T}-1} \{e^2(k) + u^2(k)\} \tag{14}$$

where $e(k)$ and $u(k)$ represent the error signal and control signal at kth sampling instant, respectively, and T_{f} represents the final time of interest.

All the simulations are performed using a personal computer with Windows 10 pro operating system, Intel Core

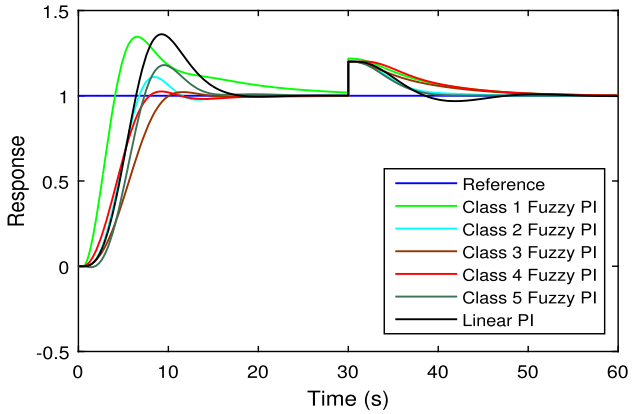

Fig. 22 Step responses of the closed loop system (Example 1)

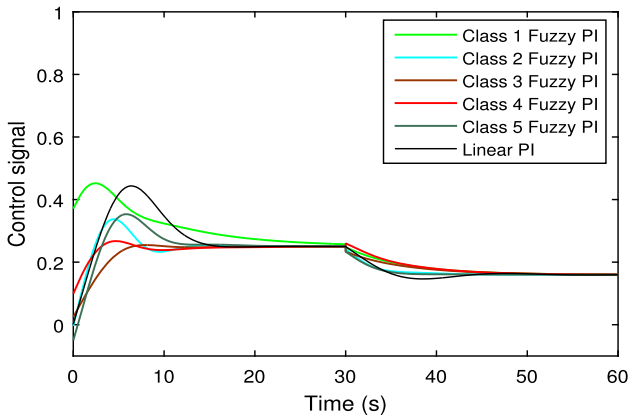

Fig. 23 Control efforts due to different PI controllers (Example 1)

i5-7500, 3.4 GHz processor, 12 GB RAM and the software package MATLAB/Simulink 8.5.0.197613 (R2015a). The ode45 (Dormand-Prince) simulation solver is used for performing the simulations. The objective function, depicted in Eq. (14), has been minimized using Genetic Algorithm (GA) for obtaining the optimal values of controller parameters. For the details of GA, one may refer to Goldberg (1989). Note that any other optimization algorithm can also be used in place of GA, but as the aim here is to show the applicability of the proposed controllers, other algorithms are not explored. The ranges of controller parameters have been fixed after a number of trial runs. At the beginning a wider solution space is considered and after getting the initial solution, the search space has been narrowed down in the subsequent steps. The final ranges of parameters used during optimization are provided in the footnotes of Tables 12, 15, 19 and 22. During optimization, population size, bit size, number of iterations, crossover probability and mutation probability are considered as 20, 10, 25, 0.8, and 0.05, respectively. Based on the complexity of a problem and desired precision, the population size, number of iterations, and bit size are usually decided. In this study, crossover probability is considered as

Table 13 Performance comparison of different PI controllers (Example 1)

Controller	MO (%)	$t_s(s)$	$t_r(s)$	e_{ss}
Class 1 Fuzzy PI	34.6	29.49	2.431	0
Class 2 Fuzzy PI	11.06	14.084	3.6430	0
Class 3 Fuzzy PI	2.15	12.155	5.63	0
Class 4 Fuzzy PI	2.52	9.96	4.6285	0
Class 5 Fuzzy PI	17.98	14.185	3.634	0
Linear PI	36.08	16.36	3.42	0
Fuzzy PI (Mudi and Pal 1999)	30.97	11.30	5.6	0
Self tuned Fuzzy PI (Mudi and Pal 1999)	25.22	14.80	5.5	0

Table 14 Performance indices of the system with different PI controllers (Example 1)

Controller	IAE	ITAE	ISE	ITSE	u_e	J
Class 1 Fuzzy PI	7.378	106.4	2.874	15.89	4.075	0.1158
Class 2 Fuzzy PI	5.908	51.83	3.818	12.48	2.778	0.1099
Class 3 Fuzzy PI	7.366	79.35	4.631	17.97	2.603	0.1206
Class 4 Fuzzy PI	6.423	83.79	3.603	15.46	2.763	0.1061
Class 5 Fuzzy PI	6.893	55.73	4.572	15.62	2.884	0.1243
Linear PI	7.674	75.64	4.392	18.16	3.4	0.1299

0.8 so that most of the parents can take part in the crossover and exchange their properties. To maintain diversity in the population, and to avoid the search turning into a primitive random search, the mutation probability is set low.

Example 1 To demonstrate the applicability of proposed simplest fuzzy PI controllers, we consider a second-order nonlinear plant with a dead-time. The corresponding differential equation governing the dynamics of the plant is as follows:

$$\ddot{y} + \dot{y} + 0.25y^2 = u(t - L) \tag{15}$$

where the system input and output are represented by $u(t)$ and $y(t)$, respectively, and $L = 0.5$ s.

Considering sampling time $T = 1ms$, GA is used to obtain the parameters of the simplest fuzzy and linear PI controllers by optimizing the cost function in Eq. (14). The fuzzy PI controller parameters are listed in Table 12. The linear PI controller parameters are obtained as $K_P^{dt} = 0.0015$ and $K_I^{dt} = 0.0001$. The value of the parameter A, for simplicity, is considered zero in the output fuzzy set for all the classes of controllers. Simulation is continued for $T_f = 60$ s. The step responses of the closed loop system along with the controller outputs due to different PI controllers are provided in Figs. 22 and 23. A step signal with amplitude 0.2, i.e. 20% of the input signal, is applied at $t = 30$ s to check the disturbance rejection ability of the proposed fuzzy PI controllers. In terms of maximum overshoot (MO), settling time (t_s), rise time (t_r) and steady state error (e_{ss}), the performance of different PI controllers are compared and the results are listed in Table 13. The performance indices like Integral Absolute Error (IAE), Integral Time Absolute Error (ITAE), Integral Squared Error (ISE), Integral Time Squared Error (ITSE), control energy ($u_e = T\sum_{k=0}^{(T_f/T)-1} u^2(k)$) and cost function ($J$) have also been found and provided in Table 14. From Fig. 22 and Table 13, we can conclude that except Class 1 controller, all other four classes of proposed controllers have the ability to control the nonlinear plant in Eq. (15) in a better way as compared to the linear PI and self tuned fuzzy PI (Mudi and Pal 1999) controllers.

Example 2 To demonstrate the applicability of proposed simplest fuzzy PD controllers, we again consider a second-order nonlinear plant with a dead-time. The corresponding differential equation governing the dynamics of the plant is as follows:

$$\ddot{y} + 0.3y\dot{y} = u(t - L) \tag{16}$$

where $u(t)$ and $y(t)$ denote the system input and output, respectively, and $L = 0.5$ s.

Considering sampling time $T = 1ms$, GA is used to obtain the controller parameters of the simplest fuzzy and linear PD controllers by optimizing the cost function in Eq. (14). The values of linear PD controller parameters are obtained as $K_P^{dt} = 0.0500$ and $K_D^{dt} = 0.0941$. For simplicity, the parameter A of the output fuzzy set is considered zero for all the classes of controllers. The optimized fuzzy PD controller parameters are summarized in Table 15.

The simulation is carried out for $T_f = 80$ s. Along with controller outputs, the unit step responses of the closed loop system due to different PD controllers are provided in Figs. 24 and 25. A step signal with amplitude 0.2, i.e. 20% of input signal, is applied at $t = 40$ s to check the disturbance rejection capability of the proposed fuzzy PD controllers. In terms of MO, t_s, t_r and e_{ss}, the performance of different PD controllers are compared and the results are provided in Table 16. IAE, ITAE, ISE, ITSE, u_e and J have also been calculated and summarized in Table 17. From Fig. 24 and

Table 15 Optimized fuzzy PD controller parameters (Class 1–Class 5, Example 2)

Parameter	Class 1	Class 2	Class 3	Class 4	Class 5
A	0	0	0	0	0
B	16.2630	15.0137	16.9941	16.9629	16.3177
h_e	79.3021	79.0039	79.1945	79.0567	79.0332
$h_{\Delta e}$	0.3746	0.3749	0.3729	0.3749	0.3741
S_e	1.6973	1.6998	1.7000	1.6967	1.6959
$S_{\Delta e}$	14.5059	14.5870	14.7170	14.5313	14.5626
S_{PD}^{-1}	8.5024	8.0762	9.9883	9.9668	8.9208

Note: During optimization, the lower and upper bounds of the parameters B, h_e, $h_{\Delta e}$, S_e, $S_{\Delta e}$, and S_{PD}^{-1} are considered as $15-17$, $79-80$, $0.365-0.375$, $1.5-1.7$, $14.5-15.5$, and $8-10$, respectively

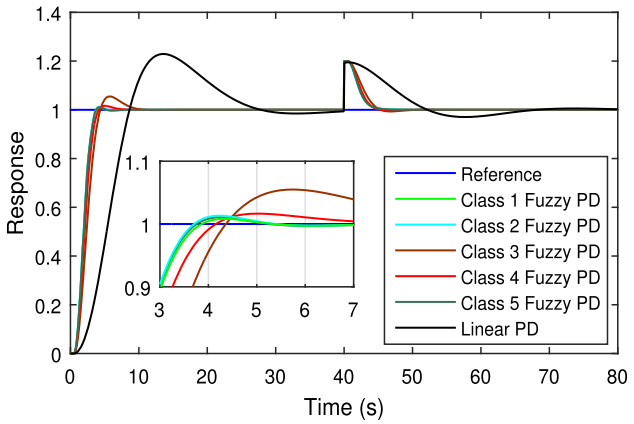

Fig. 24 Step responses of the closed loop system (Example 2)

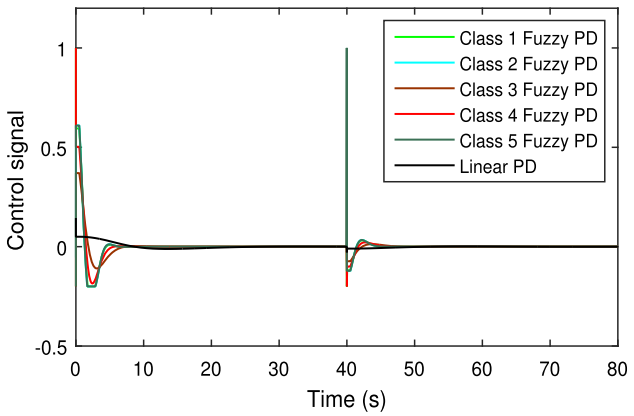

Fig. 25 Control efforts due to different PD controllers (Example 2)

Table 16, we can conclude that the proposed fuzzy PD controllers have better control ability as compared to the linear PD and self tuned fuzzy PD (Mudi and Pal 1999) controllers in controlling the nonlinear plant in Eq. (16).

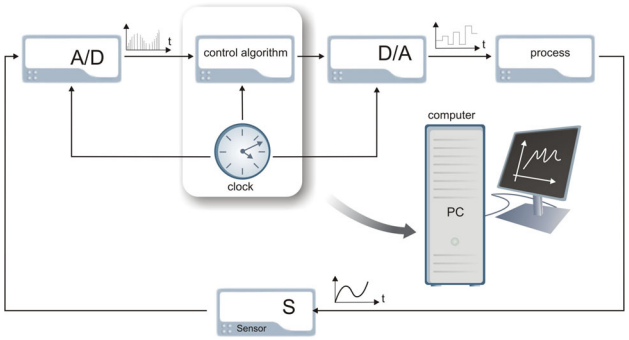

Fig. 26 Digital control system diagram

8 Real-time study

In this section, with the help of two nonlinear Single Input Single Output (SISO) plants, the real-time application of the proposed fuzzy PI/PD controllers is studied. In the first example a coupled tanks system with model no. 33-230 from Feedback Instruments is considered for showing the applicability of the proposed fuzzy PI controllers. Whereas, a Magnetic levitation (Maglev) system with model no. 33-210 from Feedback Instruments is considered in the second example for showing the applicability of the proposed fuzzy PD controllers. Apart from simulation examples, the purpose of providing the real-time studies is to comprehend the applicability of the proposed fuzzy controllers in a more realistic sense.

The digital control diagram used for performing the real-time control of both the examples is depicted in Fig. 26 (Coupled 2011b). The real-time digital control system consists of four main elements which are PC with a clocked control algorithm, analog to digital (A/D) and digital to analog (D/A) converters - serving as an interface between external environment and the PC, controlled process and sensor. The control algorithm and the A/D and D/A converters work depending on the time pulses generated by the clock.

Sampling time is defined as the time duration between two consecutive time pulses. When the clock delivers an interrupt, an interrupt service routine is called. During the interrupt service routine, an A/D converter provides a discrete representation of the sensor measurement. Based on the measurement, the control signal value is calculated via the control algorithm. At the end of the interrupt service routine, the control signal value is updated and set by the D/A converter to be held for the next sampling interval.

Example 3 Control of liquid level in a tank is considered as one of the most important issues in the process control industries. In order to ensure safety in production and quality and quantity of products, effective and timely control of liquid level is essential. In this study, we aim to control the water level of a single tank with the help of proposed fuzzy PI con-

Table 16 Performance comparison of different PD controllers (Example 2)

Controller	MO (%)	$t_s(s)$	$t_r(s)$	e_{ss}
Class 1 Fuzzy PD	0.82	3.554	1.945	0
Class 2 Fuzzy PD	1.33	3.464	1.909	0
Class 3 Fuzzy PD	5.49	8.130	2.438	0
Class 4 Fuzzy PI	1.65	3.852	2.127	0
Class 5 Fuzzy PD	1.06	3.494	1.920	0
Linear PD	22.91	25.60	5.295	0
Fuzzy PD (Mudi and Pal 1999)	30.31	8.6	2.8	0
Self tuned Fuzzy PD (Mudi and Pal 1999)	15.49	7.6	2.8	0

Table 17 Performance indices of the system with different PD controllers (Example 2)

Controller	IAE	ITAE	ISE	ITSE	u_e	J
Class 1 Fuzzy PD	2.461	21.06	1.651	4.153	0.3586	0.02512
Class 2 Fuzzy PD	2.441	21	1.635	4.113	0.375	0.02513
Class 3 Fuzzy PD	3.134	27.77	1.981	5.46	0.1567	0.02672
Class 4 Fuzzy PD	2.646	22.42	1.758	4.544	0.267	0.02531
Class 5 Fuzzy PD	2.446	21.07	1.638	4.125	0.372	0.02512
Linear PD	9.337	134.8	4.704	25.54	0.01177	0.05895

Table 18 Single tank parameters

Parameter	Value
η_t	2.2×10^{-3} ms^{-1}V^{-1}
A_t	0.01389 m^2
a_t	50.265×10^{-6} m^2
g	9.81 m/s^2

trollers. The nonlinear dynamics relating the water level h_1 and the voltage u_p applied to the pump is given by

$$\dot{h}_1(t) = \eta_t u_p(t) - \frac{a_t}{A_t}\sqrt{2gh_1(t)} \tag{17}$$

where h_1, η_t, u_p, A_t, a_t, and g, respectively, represent water level in tank, a constant relating the control voltage with the water flow from pump, voltage applied to pump, cross-sectional area of the tank, tank outlet area and acceleration due to gravity.

In Table 18, the parameters of the single tank system are provided and the real-time set-up for the water level control system is depicted in Fig. 27.

For performing the real time experimentation, we have considered the sampling time $T = 0.1$ s. With the help of GA, the proposed fuzzy PI controller parameters are found by optimizing the cost function in Eq. (14) and listed in Table 19. For simplicity the following assumptions are made: $A = 0$ and $h_e = h_{\Delta e}$. The DT linear PI controller parameters are considered as $K_P^{dt} = 100$ and $K_I^{dt} = 0.1$ (Coupled 2011a)

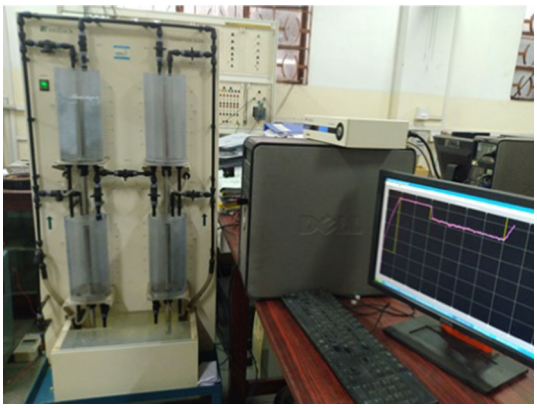

Fig. 27 Water level control system real-time set-up

which is equivalent to consider $K_P^{ct} = 100$ and $K_I^{ct} = 1$ for the CT linear PI controller.

Considering a multi-step signal as reference, the real-time experimentation is continued for $T_f = 500$ s. The first 46 seconds have been spared to bring the water level near to the operating point by applying maximum voltage (5V) to the pump. Once the response reaches the desired level, fuzzy PI controller starts to operate. The closed loop responses of the system along with control efforts due to different PI controllers are depicted in Figs. 28, 29, 30, 31, 32, 33, 34.

To check the disturbance rejection ability of the proposed fuzzy PI controllers, disturbance tap has been opened from 200 to 250 s. Performance indices like IAE, ITAE, ISE, ITSE, u_e and J for the water level control system have been obtained and summarized in Table 20. From Fig. 28 and Table 20, we

Table 19 Optimized fuzzy PI controller parameters (Class 1–Class 5, Example 3)

Parameter	Class 1	Class 2	Class 3	Class 4	Class 5
A	0	0	0	0	0
B	204.0323	203.9932	195.2346	204.9316	204.8729
h_e	19.1202	19.0059	21.1085	19.0235	19.0381
S_e	1.9076	1.9170	1.9152	1.9012	1.9047
$S_{\Delta e}$	99.8925	99.6970	99.5259	99.8338	100
S_{PI}^{-1}	1.0479	1.0480	0.9504	1.0450	1.0428

During optimization, the lower and upper bounds of the parameters B, h_e, S_e, $S_{\Delta e}$, and S_{PI}^{-1} are considered as $195-205$, $19-22$, $1.9-2.1$, $95-100$, and $0.95-1.05$, respectively

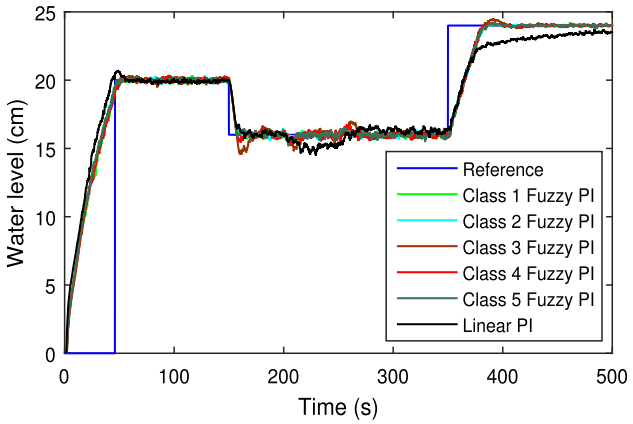

Fig. 28 Responses of water level control system with different PI controllers (Example 3)

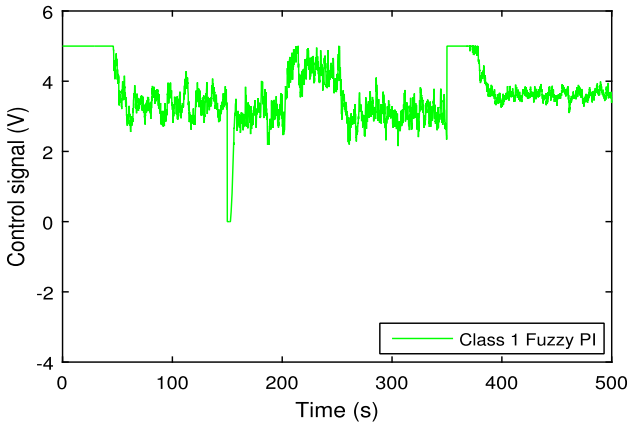

Fig. 29 Control effort of Class 1 fuzzy PI controller (Example 3)

can observe that in terms of performance and disturbance rejection ability, the proposed fuzzy PI controllers outperform linear PI controller.

Example 4 Maglev techniques have gained immense popularity over the years because of their environment friendly and cost-effective approaches, and applied successfully in different fields of research such as high-speed transportation system, industrial furnaces, energy generating units of wind turbines, biomedical instrumentation, spacecraft and

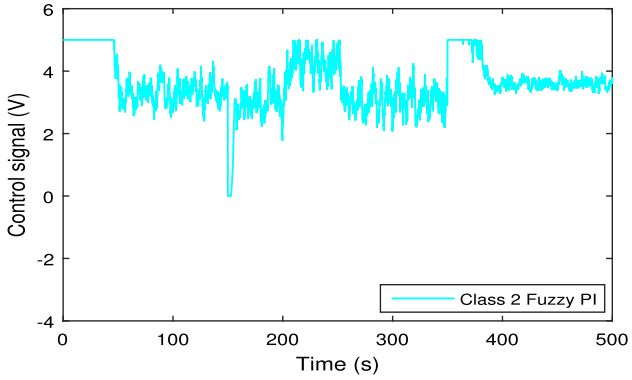

Fig. 30 Control effort of Class 2 fuzzy PI controller (Example 3)

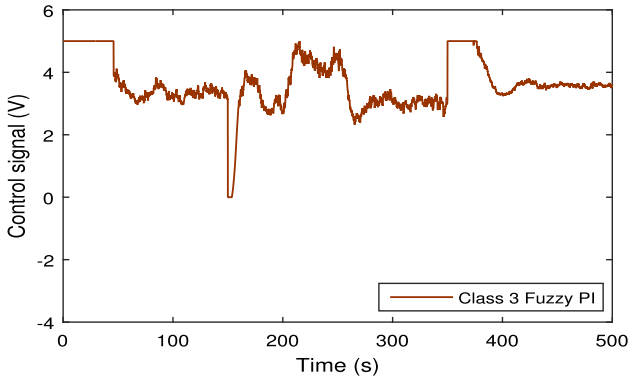

Fig. 31 Control effort of Class 3 fuzzy PI controller (Example 3)

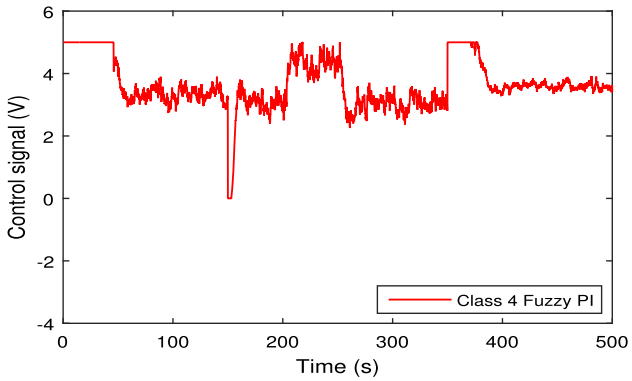

Fig. 32 Control effort of Class 4 fuzzy PI controller (Example 3)

Table 20 Performance indices of the water level control system with different PI controllers (Example 3)

Controller	IAE	ITAE	ISE	ITSE	u_e	J
Class 1 Fuzzy PI	698.9	7.136×10^4	7737	4.69×10^5	7000	29.47
Class 2 Fuzzy PI	716.7	7.294×10^4	8142	4.889×10^5	6923	30.13
Class 3 Fuzzy PI	746.6	8.043×10^4	8014	4.885×10^5	6926	29.88
Class 4 Fuzzy PI	709.3	7.328×10^4	7845	4.75×10^5	6952	29.6
Class 5 Fuzzy PI	713.7	7.229×10^4	8144	4.819×10^5	6881	30.05
Linear PI	917.7	1.289×10^5	9555	5.677×10^5	6625	32.36

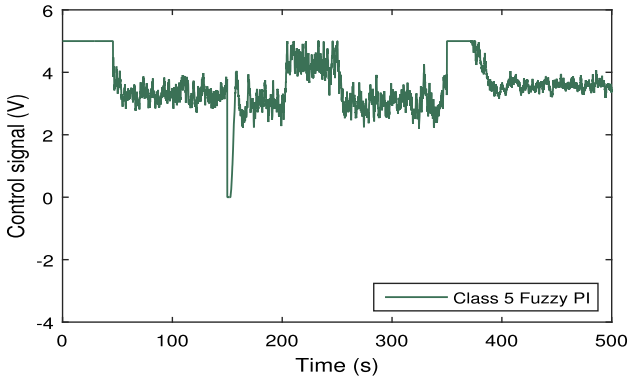

Fig. 33 Control effort of Class 5 fuzzy PI controller (Example 3)

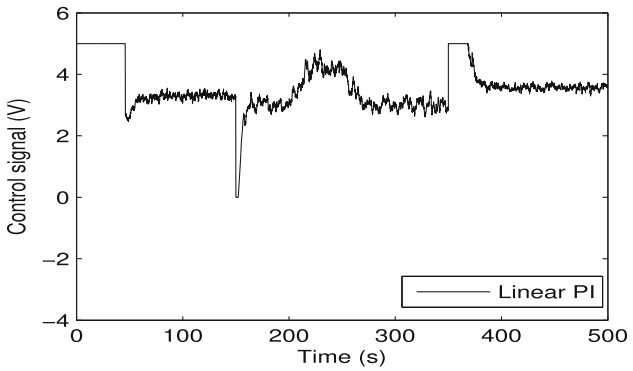

Fig. 34 Control effort of linear PI controller (Example 3)

rocket launching systems etc. Because of such extensive applications, it becomes an important task for the control system practitioners to develop a proper control strategy which can control the Maglev system efficiently. Because of its nonlinear and unstable behaviour, the control task becomes extremely difficult. From literature we find that different control strategies such as 1 and 2 Degree of Freedom (DOF) control (Ghosh et al. 2014), integer and fractional order control (Sain et al. 2016; Swain et al. 2017) etc. have been used for the purpose of controlling the Maglev system. In this study, we make an attempt to design the proposed fuzzy PD controllers for the control of Maglev system in real-time. The

Table 21 Maglev system parameter details (Swain et al. 2017)

Parameter	Value
Mass of the steel ball (m)	0.02 kg
Acceleration due to gravity (g)	9.81 m/s^2
Equilibrium value of current (i_0)	0.8 A
Equilibrium value of position (x_0)	0.009 m
Control voltage to coil current gain (k_c)	1.05 A/V
Sensor gain (k_s), offset (η)	143.48 V/m, -2.8 V
Control voltage input level (u)	$\pm$ 5 V
Sensor output voltage level (x_v)	+ 1.25 V to -3.75V

nonlinear dynamics of the Maglev system is given by

$$m\ddot{x} = mg - ki^2x^{-2} \tag{18}$$

where m, x, g and i, respectively, represent the mass of the ball, ball position, acceleration due to gravity and coil current, and k is a constant and its value depends on coil (electromagnet) parameters.

The Maglev system parameters are listed in Table 21 (Swain et al. 2017). The schematic diagram and real-time Maglev control set-up is depicted in Figs. 35 and 36.

The fuzzy PD controller parameters are obtained by optimizing the cost function in Eq. (14) with the help of GA and provided in Table 22. The sampling time is considered as 1 ms. For simplicity the value of parameter $h_{\Delta e}$ is considered same as h_e i.e. $h_e = h_{\Delta e}$. Utilizing the same cost function as depicted in Eq. (14), using GA, the linear PD controller parameters are obtained as $K_P^{dt} = 3.7$ and $K_D^{dt} = 96.8$ which is equivalent to consider $K_P^{ct} = 3.7$ and $K_D^{ct} = 0.0968$ for the CT linear PD controller.

The real-time experimentation has been performed for $T_f = 45$ s where a square wave is chosen as the reference signal. From the linearized model of the Maglev system we observe that it is a type zero system and occurrence of steady state error with PD controller is natural. A gain block has been inserted after the reference signal to reduce the steady state error. Along with the control efforts, the closed loop responses of the Maglev system due to different PD controllers are provided in Figs. 37, 38, 39, 40, 41, 42, 43, 44. In

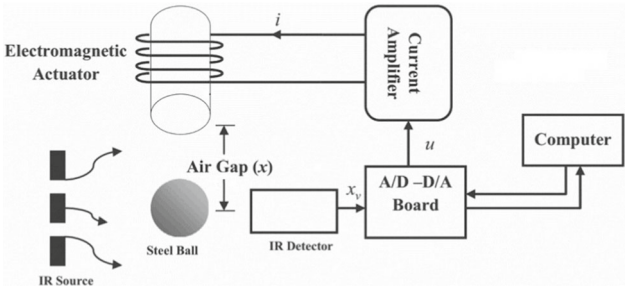

Fig. 35 Schematic diagram of the Maglev system

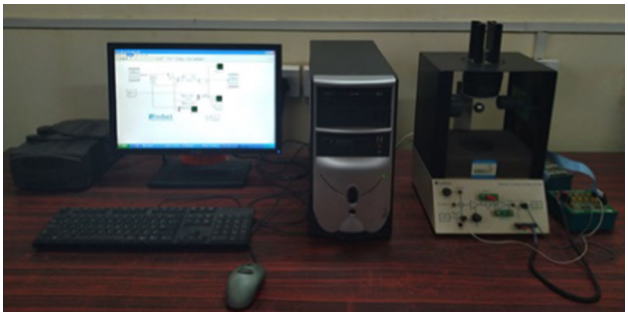

Fig. 36 Real-time control set-up of the Maglev system

Table 22 Optimized parameters of fuzzy PD controllers (Classes 1-5, Example 4)

Parameter	Class 1	Class 2	Class 3	Class 4	Class 5
A	0.5043	0.5090	0.5095	0.5086	0.5059
B	1.0495	1.0467	1.0479	1.0483	1.0496
h_e	0.1852	0.1850	0.1852	0.1850	0.1851
S_e	0.8954	0.8935	0.8987	0.8981	0.8982
$S_{\Delta e}$	15.0434	15.0237	15.0403	15.0011	14.9567
S_{PD}^{-1}	2.8963	2.8995	2.8974	2.8945	2.8988

During optimization, the lower and upper bounds of the parameters A, B, h_e, S_e, $S_{\Delta e}$, and S_{PD}^{-1} are considered as $0.49 - 0.51$, $0.95 - 1.05$, $0.185 - 0.195$, $0.85 - 0.9$, $14.95 - 15.05$, and $2.85 - 2.9$, respectively

the graphs we have indicated the ball position in volts as the position of the ball gets converted into an equivalent voltage signal. The response of the Maglev system with Class 3 fuzzy PD controller is provided separately along with the response due to linear PD controller in Fig. 38 because of the presence of comparatively large oscillations as compared to other fuzzy PD controllers. We notice that except for Class 4 fuzzy and linear PD controllers, the control effort is in the permissible range i.e. in between ±5V. Before applying the controller output to the plant, in general the control signal is passed through a saturation block to restrict the high amplitude of the control signal, if any, for the purpose of plant safety. From the response of closed loop Maglev system, IAE, ITAE, ISE, ITSE, u_e and J have been found and summarized in Table 23. From Table 23, it is found that in

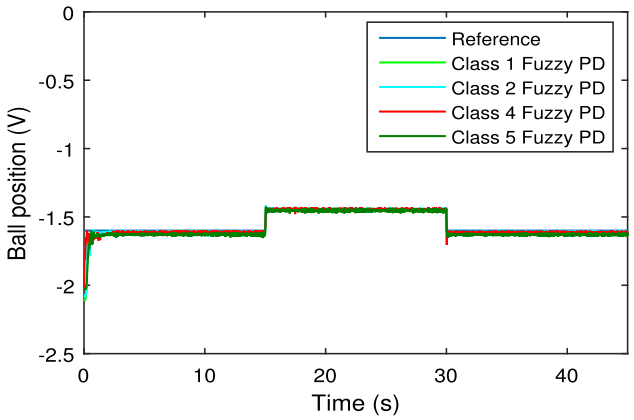

Fig. 37 Closed loop responses of Maglev system with different fuzzy PD controllers (Classes 1, 2, 4 and 5, Example 4)

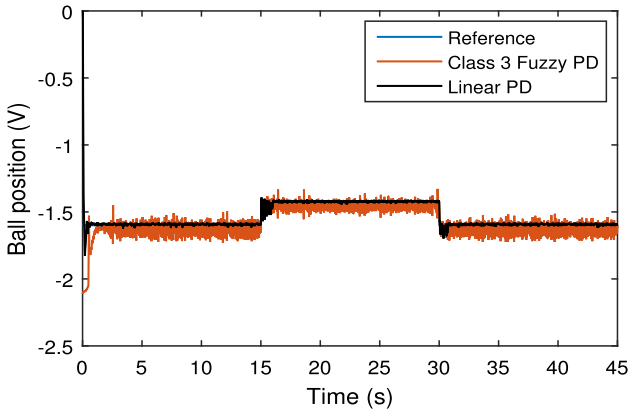

Fig. 38 Closed loop response of Maglev system with Class 3 fuzzy and linear PD controller (Example 4)

terms of IAE, ITAE, ISE, and ITSE, the Class 1, Class 2 and Class 4 fuzzy PD controllers outperform Class 3 and Class 5 fuzzy PD and linear PD controllers. Moreover, it is also observed that in terms of control energy and cost function value, the proposed fuzzy PD controllers outperform the linear PD controller.

During the real-time experimentation, between 15 and 20 s hand held disturbance has been applied to check the robustness capability of the proposed fuzzy PD controllers. Moreover, for better understanding, input and output disturbances have also been applied simultaneously. A step signal with an amplitude 0.155 V i.e. 10 % of the average value of the reference signal has been considered as input disturbance and as output disturbance a pulse signal with an amplitude 0.31 V i.e. 20 % of the average value of the reference signal and a period of 12 s has been considered. We observe that except Class 3 fuzzy PD controller, all other classes of fuzzy PD controllers can withstand these simultaneous input and output disturbances. By reducing both input and output disturbances by a factor of two, we notice that Maglev system with Class 3 fuzzy PD controller can also withstand input

Table 23 Performance indices of the Maglev system with different PD controllers (Example 4)

Controller	IAE	ITAE	ISE	ITSE	u_e	J
Class 1 Fuzzy PD	0.6838	12.18	0.06921	0.2045	19.37	0.432
Class 2 Fuzzy PD	0.6772	11.8	0.06866	0.1938	22.17	0.4941
Class 3 Fuzzy PD	1.78	34.14	0.2084	1.843	39.13	0.8742
Class 4 Fuzzy PD	0.5938	11.73	0.02039	0.1865	9.344	0.2081
Class 5 Fuzzy PD	1.116	22.13	0.08085	0.6479	31.88	0.7102
Linear PD	0.8221	15.67	0.1658	0.3822	55.96	1.247

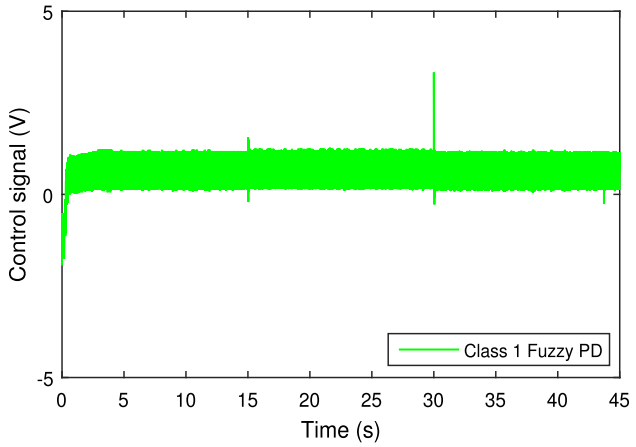

Fig. 39 Class 1 fuzzy PD controller output (Example 4)

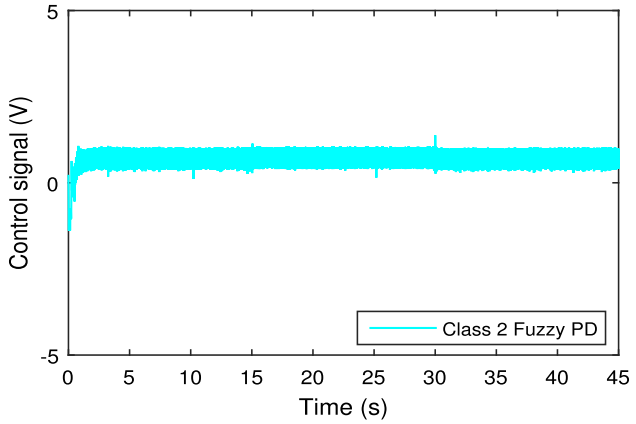

Fig. 40 Class 2 fuzzy PD controller output (Example 4)

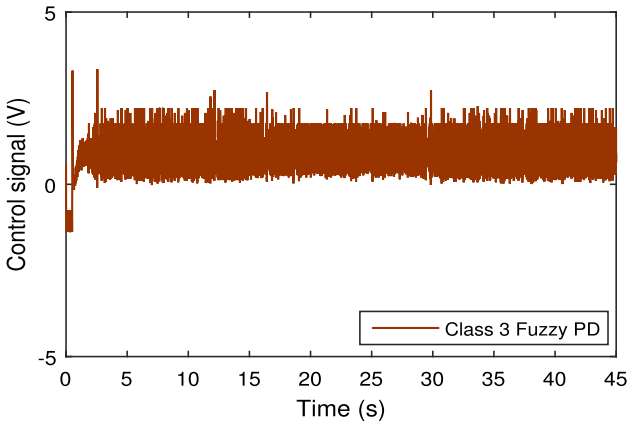

Fig. 41 Class 3 fuzzy PD controller output (Example 4)

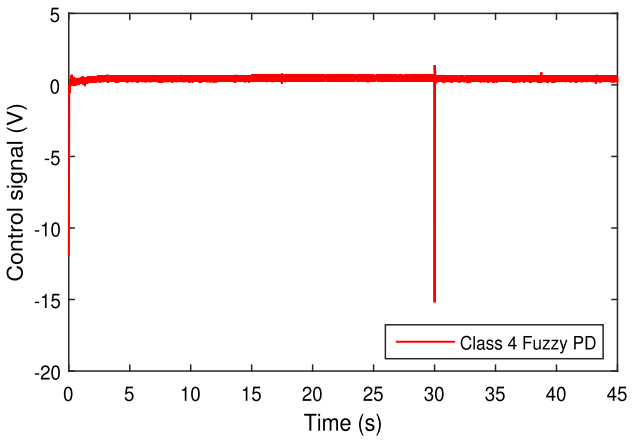

Fig. 42 Class 4 fuzzy PD controller output (Example 4)

and output disturbances. The closed loop responses of the Maglev system in presence of different disturbances are provided in Figs. 45, 46, 47, 48 which confirm the robustness of the proposed fuzzy PD controllers.

In spite of using the gain block after the reference signal it can be observed from Figs. 47 and 48 that the steady state error has comparatively increased. This is because of the input disturbance signal which changes the level of control signal continuously. With the help of a PID controller the issues related to the steady state error can be handled efficiently. We plan to do this in near future. It has further been noticed that the Maglev system with linear PD controller can withstand the hand held and input disturbances, but not the output pulse disturbance. In presence of the hand held, and input disturbances the responses of the closed loop Maglev system with linear PD controller are provided in Figs. 49 and 50, respectively.

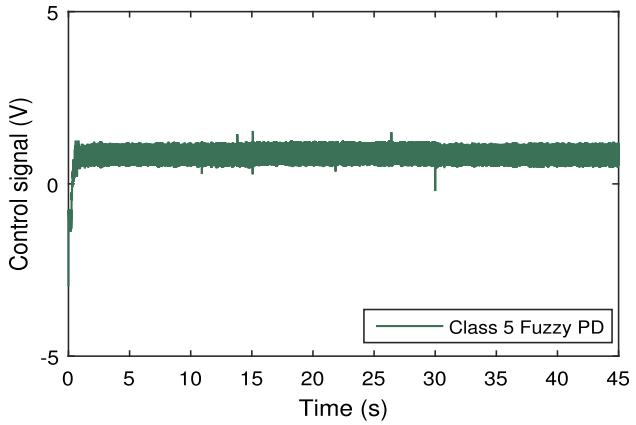

Fig. 43 Class 5 fuzzy PD controller output (Example 4)

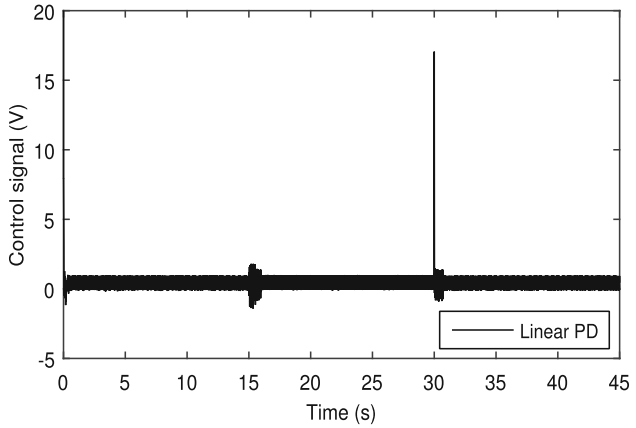

Fig. 44 Conventional linear PD controller output (Example 4)

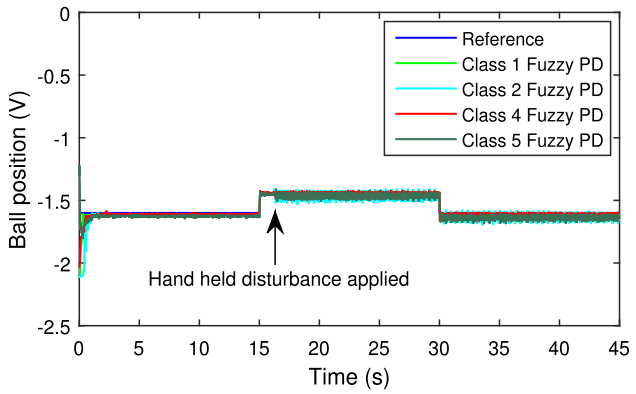

Fig. 45 Closed loop responses of Maglev system in presence of hand held disturbance (Classes 1, 2, 4 and 5 fuzzy PD controllers, Example 4)

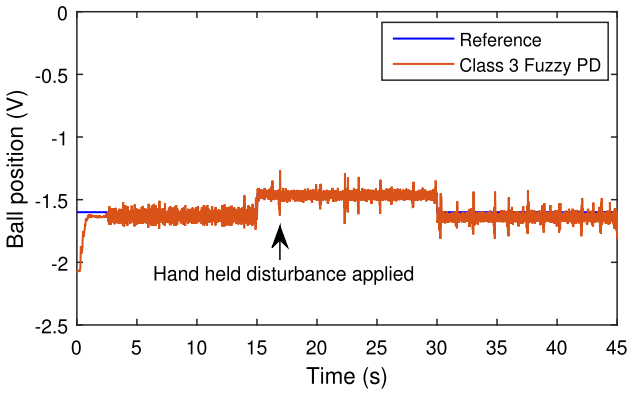

Fig. 46 Closed loop response of Maglev system in presence of hand held disturbance (Class 3 fuzzy PD controller, Example 4)

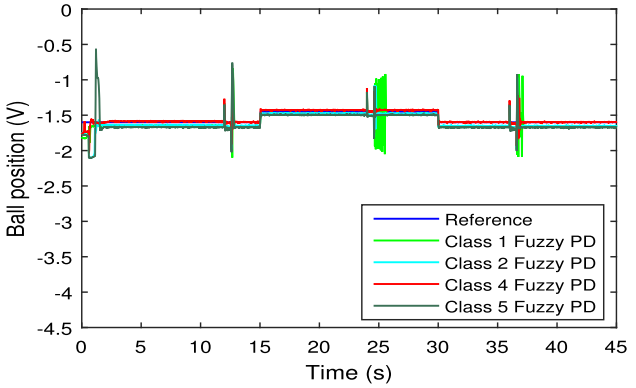

Fig. 47 Closed loop responses of Maglev system in presence of both input and output disturbances (Classes 1, 2, 4 and 5 fuzzy PD controllers, Example 4)

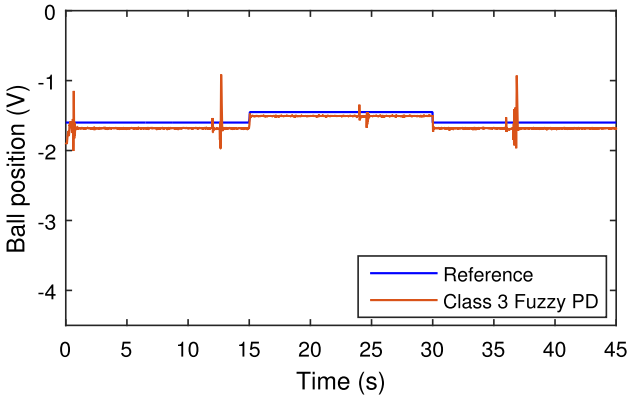

Fig. 48 Closed loop response of Maglev system in presence of reduced input and output disturbances (Class 3 fuzzy PD controller, Example 4)

9 Conclusions

In this paper, the exact analytical structures of five new simplest fuzzy PI/PD controllers are obtained using CoG defuzzification. Properties and computational aspects of the proposed fuzzy PI/PD controllers are studied, and sufficient conditions for the stability of a closed loop system containing one of the controllers in the loop are established using the Small-Gain theorem. For better understanding, the applicability of the proposed simplest fuzzy PI/PD controllers is substantiated through simulation and real-time studies. In future, as a further scope of research, other optimization

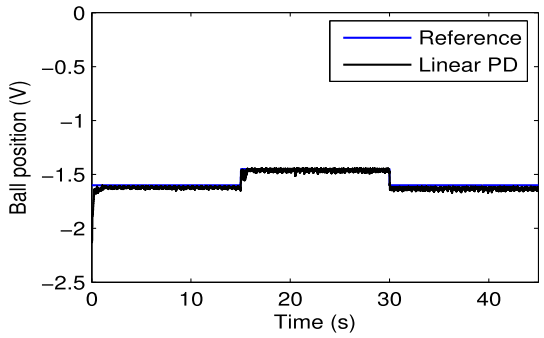

Fig. 49 Closed loop response of the Maglev system in presence of hand held disturbance (DT linear PD controller, Example 4)

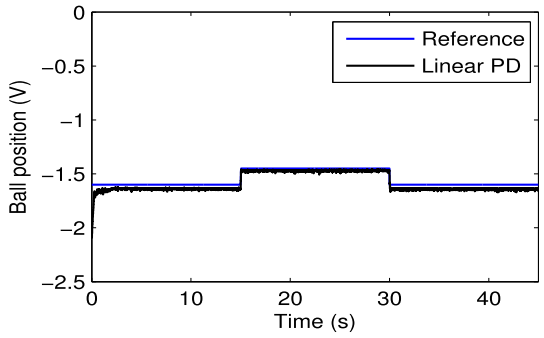

Fig. 50 Closed loop response of the Maglev system in presence of input disturbance (DT linear PD controller, Example 4)

algorithms will be explored for the design of proposed fuzzy PI/PD controllers and the performances of the proposed controllers will be compared with that of the other controllers already reported in the literature. Moreover, for ensuring stability, BIBO stability conditions obtained in this study can also be utilized for the design of proposed fuzzy controllers.

Declarations

Conflict of interest The authors declare that they have no conflict of interest.

Ethical approval This article does not contain any studies with human participants or animals performed by any of the authors.

Informed consent Informed consent was obtained from all individual participants included in the study.

References

Arun NK, Mohan BM (2017) Modeling, stability analysis, and computational aspects of some simplest nonlinear fuzzy two-term controllers derived via center of area/gravity defuzzification. ISA Trans 70:16–29

Braae M, Rutherford D (1979) Selection of parameters for a fuzzy logic controller. Fuzzy Sets Syst 2(3):185–199

Coupled Tanks (2011) Control experiments. Feedback Instruments Limited, UK

Coupled Tanks (2011) Installation Commissioning. Feedback Instruments Limited, UK

Driankov D, Hellendoorn H, Reinfrank M (1993) An introduction to fuzzy control. Springer, Berlin

Du X, Ying H (2010) Derivation and analysis of the analytical structures of the interval type-2 fuzzy-PI and PD controllers. IEEE Trans Fuzzy Syst 18(4):802–814

Ghosh A, Krishnan TR, Tejaswy P, Mandal A, Pradhan JK, Ranasingh S (2014) Design and implementation of a 2-DOF PID compensation for magnetic levitation systems. ISA Trans 53(4):1216–1222

Goldberg DE (1989) Genetic algorithms in search. Optimization and machine learning. Pearson Education, Chennai

Haj-Ali A, Ying H (2003) Input-output structural relationship between fuzzy controllers using nonlinear input fuzzy sets and PI or PD control. Int J Fuzzy Syst 5(1):60–65

Khalil HK (2015) Nonlinear control. Pearson Education Ltd, London

Klement EP, Mesiar R, Pap E (2000) Triangular norms. Kluwer Academic Publishers, Boston

Malki HA, Li H, Chen G (1994) New design and stability analysis of fuzzy proportional-derivative control systems. IEEE Trans Fuzzy Syst 2(4):245–254

Mamdani EH (1974) Application of fuzzy algorithms for control of simple dynamic plant. Proc Inst Electr Eng 121(12):1585–1588

Mohan BM, Patel AV (2002) Analytical structures and analysis of the simplest fuzzy PD controllers. IEEE Trans Syst Man Cybern Part B Cybern 32(2):239–248

Mohan BM, Sinha A (2008) Mathematical models of the simplest fuzzy PI/PD controllers with skewed input and output fuzzy sets. ISA Trans 47(3):300–310

Mudi RK, Pal NR (1999) A robust self-tuning scheme for PI-and PD-type fuzzy controllers. IEEE Trans Fuzzy Syst 7(1):2–16

Neelimegham KMA, Bosukonda MM (2015) Mathematical modeling and computational study of the simplest fuzzy two-term controllers via height defuzzification. J Intell Fuzzy Syst 29(5):1817–1826

Nie M, Tan WW (2012) Analytical structure and characteristics of symmetric Karnik–Mendel type-reduced interval type-2 fuzzy PI and PD controllers. IEEE Trans Fuzzy Syst 20(3):416–430

Patel AV, Mohan BM (2002) Analytical structures and analysis of the simplest fuzzy PI controllers. Automatica 38(6):981–993

Raj R, Mohan BM (2019) Analytical structures and stability analysis of the simplest Takagi–Sugeno fuzzy two-term controllers. Int J Process Syst Eng 5(1):67–92

Raj R, Mohan BM (2020) General structure of interval type-2 fuzzy PI/PD controller of Takagi–Sugeno type. Eng Appl Artif Intell 87:103273

Sain D, Swain SK, Mishra SK (2016) TID and I-TD controller design for magnetic levitation system using genetic algorithm. Perspect Sci 8:370–373

Swain SK, Sain D, Mishra SK, Ghosh S (2017) Real time implementation of fractional order PID controllers for a magnetic levitation plant. AEU Int J Electron Commun 78:141–156

Ying H (1993) The simplest fuzzy controllers using different inference methods are different nonlinear proportional-integral controllers with variable gains. Automatica 29(6):1579–1589

Ying H (2000) Fuzzy control and modeling: analytical foundations and applications. Wiley-IEEE Press, Hoboken

Ying H, Siler W, Buckley JJ (1990) Fuzzy control theory: a nonlinear case. Automatica 26(3):513–520

Yip CMT, Tan WW, Nie M (2019) On the difference in control performance of interval type-2 fuzzy PI control system with different FOU shapes. Appl Soft Comput 76:517–532

Zadeh LA (1965) Fuzzy sets. Inf Control 8(3):338–353

Zadeh LA (1972) A rationale for fuzzy control. J Dyn Syst Meas Control 94(1):3–4

Zhou H, Zhang C, Tan S, Dai Y, Duan J (2020) Design of the footprints of uncertainty for a class of typical interval type-2 fuzzy PI and PD controllers. ISA Trans